



NRL/MR/6110--10-9289

# EMI Array for Cued UXO Discrimination

## ESTCP MM-0601

### Final Report

D.C. GEORGE

*G&G Sciences*

*Grand Junction, Colorado*

J.B. KINGDON

T. FURUYA

D.A. KEISWETTER

T.H. BELL

*SAIC, Inc. - ASAD*

*Arlington, Virginia*

G.R. HARBAUGH

D.A. STEINHURST

*Nova Research, Inc.*

*Alexandria, Virginia*

September 16, 2010

REPORT DOCUMENTATION PAGE				Form Approved OMB No. 0704-0188	
Public reporting burden for this collection of information is estimated to average 1 hour per response, including the time for reviewing instructions, searching existing data sources, gathering and maintaining the data needed, and completing and reviewing this collection of information. Send comments regarding this burden estimate or any other aspect of this collection of information, including suggestions for reducing this burden to Department of Defense, Washington Headquarters Services, Directorate for Information Operations and Reports (0704-0188), 1215 Jefferson Davis Highway, Suite 1204, Arlington, VA 22202-4302. Respondents should be aware that notwithstanding any other provision of law, no person shall be subject to any penalty for failing to comply with a collection of information if it does not display a currently valid OMB control number. <b>PLEASE DO NOT RETURN YOUR FORM TO THE ABOVE ADDRESS.</b>					
1. REPORT DATE (DD-MM-YYYY) 16-09-2010		2. REPORT TYPE Final Report		3. DATES COVERED (From - To)	
4. TITLE AND SUBTITLE  EMI Array for Cued UXO Discrimination ESTCP MM-0601 Final Report				5a. CONTRACT NUMBER	
				5b. GRANT NUMBER	
				5c. PROGRAM ELEMENT NUMBER	
6. AUTHOR(S)  D.C. George,* J.B. Kingdon,† T. Furuya,‡ D.A. Keiswetter,† T.H. Bell,† G.R. Harbaugh,‡ and D.A. Steinhurst‡				5d. PROJECT NUMBER MM-0601	
				5e. TASK NUMBER	
				5f. WORK UNIT NUMBER 61-5802-P-0	
7. PERFORMING ORGANIZATION NAME(S) AND ADDRESS(ES)  Naval Research Laboratory, Code 6110 4555 Overlook Avenue, SW Washington, DC 20375-5320				8. PERFORMING ORGANIZATION REPORT NUMBER  NRL/MR/6110--10-9289	
9. SPONSORING / MONITORING AGENCY NAME(S) AND ADDRESS(ES)  Environmental Security Technology Certification Program (ESTCP) Program Office 901 North Stuart Street, Suite 303 Arlington, VA 22203				10. SPONSOR / MONITOR'S ACRONYM(S) ESTCP	
				11. SPONSOR / MONITOR'S REPORT NUMBER(S)	
12. DISTRIBUTION / AVAILABILITY STATEMENT  Approved for public release; distribution is unlimited.					
13. SUPPLEMENTARY NOTES *G&G Sciences, 873 23 Road, Grand Junction, CO 81505 †SAIC, Inc. - ASAD, 1225 South Clark Street, Suite 800, Arlington, VA 22202 ‡Nova Research, Inc., 1900 Elkin Street, Suite 230, Alexandria, VA 22308					
14. ABSTRACT  A vehicle-towed array of time-domain electromagnetic sensors was designed and operated to optimize the classification of buried munitions from ancillary metallic debris and clutter. The array was designed to combine the data quality advantages of a gridded survey with the coverage efficiencies of a vehicular system. The design goal for this system was to collect data equal, if not better, in quality to the best gridded surveys while prosecuting many more targets each field day. In order to separate out the intrinsic target response properties from sensor/target geometry effects, the measured signature is inverted to estimate principal axis magnetic polarizabilities using a standard induced dipole response model. The technology was validated through two blind tests conducted at the Aberdeen Proving Ground Standardized UXO Test Site and as part of the ESTCP UXO Classification Study at the former Camp San Luis Obispo. The performance metrics used to monitor the success of the technology relate to production rate, accuracy of inverted features, analysis time, correct classification, and ease of use.					
15. SUBJECT TERMS Discrimination      Unexploded Ordnance (UXO)      Electromagnetic Induction (EMI) Classification      Multi-sensor Towed Array Detection System (MTADS)      Magnetometry					
16. SECURITY CLASSIFICATION OF:			17. LIMITATION OF ABSTRACT  UL	18. NUMBER OF PAGES  91	19a. NAME OF RESPONSIBLE PERSON B.J. Spargo, NRL, Code 6110
a. REPORT Unclassified	b. ABSTRACT Unclassified	c. THIS PAGE Unclassified			19b. TELEPHONE NUMBER (include area code) (202) 404-6392

## Contents

Figures.....	xi
Tables.....	xiii
Acronyms.....	xv
Acknowledgements.....	xvi
EXECUTIVE SUMMARY .....	E-1
1.0 Introduction.....	1
1.1 Background .....	1
1.2 Objective of the Demonstration .....	1
1.3 Regulatory Drivers .....	2
2.0 Technology .....	2
2.1 Technology Description .....	2
2.1.1 EMI Sensors.....	2
2.1.2 Sensor Array .....	3
2.1.3 Application of the Technology .....	5
2.2 Technology Development .....	5
2.3 Advantages and Limitations of the Technology .....	11
3.0 Performance Objectives .....	12
3.1 APG Standardized UXO Test Site .....	12
3.1.1 Objective: Reduction of False Alarms.....	13
3.1.1.1. Metric .....	13
3.1.1.2. Data Requirements .....	13
3.1.1.3. Success Criteria.....	13
3.1.1.4. Results .....	13

3.1.2	Objective: Location Accuracy .....	13
3.1.2.1.	Metric .....	14
3.1.2.2.	Data Requirements .....	14
3.1.2.3.	Success Criteria .....	14
3.1.2.4.	Results .....	14
3.1.3	Objective: Production Rate.....	14
3.1.3.1.	Metric .....	14
3.1.3.2.	Data Requirements .....	14
3.1.3.3.	Success Criteria .....	14
3.1.3.4.	Results .....	15
3.1.4	Objective: Analysis Time .....	15
3.1.4.1.	Metric .....	15
3.1.4.2.	Data Requirements .....	15
3.1.4.3.	Success Criteria .....	15
3.1.4.4.	Results .....	15
3.1.5	Objective: Ease of Use .....	15
3.1.5.1.	Data Requirements .....	15
3.1.5.2.	Results .....	16
3.2	Former Camp San Luis Obispo.....	17
3.2.1	Objective: Site Coverage.....	17
3.2.1.1.	Metric .....	18
3.2.1.2.	Data Requirements .....	18
3.2.1.3.	Success Criteria .....	18
3.2.1.4.	Results .....	18

3.2.2	Objective: Calibration Strip Results .....	18
3.2.2.1.	Metric .....	18
3.2.2.2.	Data Requirements .....	18
3.2.2.3.	Success Criteria .....	18
3.2.2.4.	Results .....	19
3.2.3	Objective: Location Accuracy .....	19
3.2.3.1.	Metric .....	19
3.2.3.2.	Data Requirements .....	19
3.2.3.3.	Success Criteria .....	19
3.2.3.4.	Results .....	19
3.2.4	Objective: Depth Accuracy .....	20
3.2.4.1.	Metric .....	20
3.2.4.2.	Data Requirements .....	20
3.2.4.3.	Success Criteria .....	20
3.2.4.4.	Results .....	20
3.2.5	Objective: Production Rate.....	20
3.2.5.1.	Metric .....	21
3.2.5.2.	Data Requirements .....	21
3.2.5.3.	Success Criteria .....	21
3.2.5.4.	Results .....	21
3.2.6	Objective: Data Throughput .....	21
3.2.6.1.	Metric .....	21
3.2.6.2.	Data Requirements .....	21
3.2.6.3.	Success Criteria .....	22

3.2.6.4.	Results .....	22
3.2.7	Objective: Reliability and Robustness.....	22
3.2.7.1.	Data Requirements .....	22
3.2.7.2.	Results .....	22
4.0	Site Description.....	22
4.1	APG Standardized UXO Technology Demonstration Site .....	23
4.1.1	Site Selection .....	23
4.1.2	Site History .....	23
4.1.3	Site Topography and Geology .....	23
4.1.4	Munitions Contamination .....	23
4.1.5	Site Geodetic Control Information .....	24
4.1.6	Site Configuration.....	24
4.2	Former Camp San Luis Obispo.....	26
4.2.1	Site Selection .....	26
4.2.2	Site History .....	26
4.2.3	Site Topography and Geology .....	27
4.2.4	Munitions Contamination .....	27
4.2.5	Site Geodetic Control Information .....	28
4.2.6	Site Configuration.....	30
5.0	Test Design .....	30
5.1	Conceptual Experimental Design.....	30
5.2	Site Preparation .....	31
5.3	Systems Specification .....	31
5.3.1	MTADS Tow Vehicle.....	31

5.3.2	RTK GPS System .....	32
5.3.3	Time-Domain Electromagnetic Sensor.....	32
5.4	Calibration Activities .....	33
5.5	Data Collection.....	35
5.5.1	Scale of Demonstration.....	35
5.5.2	Sample Density .....	36
5.5.3	Quality Checks.....	36
5.5.4	Data Handling .....	40
5.5.5	APG Discrimination Survey Data Summary .....	40
5.5.5.1.	Calibration Area .....	41
5.5.5.2.	Blind Grid.....	41
5.5.5.3.	Indirect Fire Area .....	41
5.5.6	Former Camp San Luis Obispo.....	41
5.5.6.1.	Calibration Strip .....	42
5.5.6.2.	Main Demonstration.....	42
5.6	Validation .....	42
5.6.1	Aberdeen Proving Grounds.....	42
5.6.2	Former Camp San Luis Obispo.....	42
6.0	Data Analysis and Products .....	42
6.1	Preprocessing .....	43
6.2	Target Selection for Detection .....	43
6.3	Parameter Estimation .....	44
6.4	Classifier and Training .....	46
6.4.1	Cannot Analyze.....	47

6.4.2	Likely Munition .....	47
6.4.3	Cannot Decide.....	47
6.4.4	Likely Clutter .....	48
6.4.5	Ranking.....	48
6.4.6	Determination of Overlapping Signals .....	48
6.5	Data Products .....	49
7.0	Performance Assessment .....	50
7.1	APG Standardized UXO Test Site .....	50
7.1.1	Objective: Reduction of False Alarms.....	51
7.1.1.1.	Metric .....	51
7.1.1.2.	Data Requirements .....	52
7.1.1.3.	Success Criteria .....	52
7.1.1.4.	Results .....	52
7.1.2	Objective: Location Accuracy .....	54
7.1.2.1.	Metric .....	54
7.1.2.2.	Data Requirements .....	54
7.1.2.3.	Success Criteria .....	54
7.1.2.4.	Results .....	55
7.1.3	Objective: Production Rate.....	55
7.1.3.1.	Metric .....	55
7.1.3.2.	Data Requirements .....	55
7.1.3.3.	Success Criteria .....	56
7.1.3.4.	Results .....	56
7.1.4	Objective: Analysis Time .....	56

7.1.4.1.	Metric .....	56
7.1.4.2.	Data Requirements .....	56
7.1.4.3.	Success Criteria .....	56
7.1.4.4.	Results .....	56
7.1.5	Objective: Ease of Use .....	57
7.1.5.1.	Data Requirements .....	57
7.1.5.2.	Results .....	57
7.2	Former Camp San Luis Obispo.....	57
7.2.1	Objective: Site Coverage .....	59
7.2.1.1.	Metric .....	59
7.2.1.2.	Data Requirements .....	59
7.2.1.3.	Success Criteria .....	59
7.2.1.4.	Results .....	59
7.2.2	Objective: Calibration Strip Results .....	59
7.2.2.1.	Metric .....	60
7.2.2.2.	Data Requirements .....	60
7.2.2.3.	Success Criteria .....	60
7.2.2.4.	Results .....	60
7.2.3	Objective: Location Accuracy .....	64
7.2.3.1.	Metric .....	64
7.2.3.2.	Data Requirements .....	64
7.2.3.3.	Success Criteria .....	64
7.2.3.4.	Results .....	65
7.2.4	Objective: Depth Accuracy .....	65

7.2.4.1.	Metric .....	65
7.2.4.2.	Data Requirements .....	65
7.2.4.3.	Success Criteria .....	65
7.2.4.4.	Results .....	65
7.2.5	Objective: Production Rate.....	66
7.2.5.1.	Metric .....	66
7.2.5.2.	Data Requirements .....	66
7.2.5.3.	Success Criteria .....	66
7.2.5.4.	Results .....	66
7.2.6	Objective: Data Throughput .....	66
7.2.6.1.	Metric .....	66
7.2.6.2.	Data Requirements .....	67
7.2.6.3.	Success Criteria .....	67
7.2.6.4.	Results .....	67
7.2.7	Objective: Reliability and Robustness.....	67
7.2.7.1.	Data Requirements .....	67
7.2.7.2.	Results .....	67
8.0	Cost Assessment .....	67
8.1	Cost Model .....	68
8.2	Cost Drivers.....	70
8.3	Cost Benefit.....	70
9.0	Implementation Issues .....	70
10.0	References.....	71
Appendix A:	Points of Contact.....	73

## Figures

Figure 2-1 – Construction details of an individual EMI sensor (left panel) and the assembled sensor with end caps attached (right panel). .....	2
Figure 2-2 – Measured transmit current (on-time upper panel, off-time second panel), full measured signal decay (third panel), and gated decay (fourth panel) as discussed in the text. ....	3
Figure 2-3 – Sketch of the EMI sensor array showing the position of the 25 sensors and the three GPS antennae. ....	4
Figure 2-4 – Sensor array mounted on the MTADS EMI sensor platform. ....	4
Figure 2-5 – Measured response from a 2-in steel sphere 25 cm from the sensor. Decays 1, 1001, 2001, and 3001 from a series that started from a cold start are plotted along with the expected response from this target.....	6
Figure 2-6 – Measured response from three calibration coils and the background response between measurements plotted on a semi-log plot to emphasize the exponential nature of the decay. The decay time constants extracted from the measurements are listed in the legend.....	7
Figure 2-7 – Comparison of the response of the array members. The measured decay from a 2-in steel sphere held 30 cm below each sensor in turn is plotted. The decays are indistinguishable. ....	8
Figure 2-8 – The response of nine of the individual sensors to a 40-mm projectile located under the center of the array. ....	9
Figure 2-9 – Derived response coefficients for a 40-mm projectile using the measurements of which the decays shown in Figure 2-8 are a subset.....	10
Figure 2-10 – Derived response coefficients from a cued measurement over "Cylinder E" in the test field.....	10
Figure 2-11 – Three sets of $\beta$ s derived from three measurements over a 4.2-in mortar baseplate at different position/orientation pairs.....	11
Figure 4-1 – Map of the reconfigured APG Standardized UXO Test Site. ....	25

Figure 4-2 – ESTCP UXO Classification Study demonstration site at the former Camp San Luis Obispo. The site is shown as a series of included 30m x 30m cells. See the text for further discussion. ....	29
Figure 4-3 – Locations of two GPS control points with respect to former Camp SLO demonstration site .....	30
Figure 5-1 – MTADS tow vehicle and magnetometer array. ....	32
Figure 5-2 – Average polarizability for all measurements at APG of the 4” Aluminum sphere as a function of decay time .....	34
Figure 5-3 – Comparison of measured (blue) versus theoretical (red) polarizability as a function of time for the 4” Aluminum sphere.....	35
Figure 5-4 – Monostatic QC contour plot for Calibration Area item I6.....	37
Figure 5-5 – Polarizability as a function of time for a 105mm HEAT Projectile with all data included. The fit coherence for all elements included was 0.699. ....	37
Figure 5-6 – Polarizability as a function of time for a 105mm HEAT Projectile with element 21 excluded. The fit coherence with element 21 excluded was 0.992.....	38
Figure 5-7 – Monostatic QC contour plot for example anomaly .....	39
Figure 5-8 – Polarizability as a function of time for the example show in Figure 5-7 with all data included. The fit coherence for all elements included was 0.652. ....	39
Figure 5-9 – Polarizability as a function of time for the example show in Figure 5-7 with elements 0,5,10,11,15,16,17,20,21,22 excluded. The fit coherence for the remaining elements was 0.985.....	40
Figure 6-1 – Principal axis polarizabilities for a ½ cm thick by 25cm long by 15cm wide mortar fragment. ....	45
Figure 7-1 – Peak signals compared with response curve for a 2.36-in rocket. ....	61
Figure 7-2 – Peak signals compared with response curve for a 4.2-in mortar.....	62
Figure 7-3 – Peak signals compared with response curve for a 60-mm mortar. ....	62
Figure 7-4 – Peak signals compared with response curve for an 81-mm mortar. ....	63
Figure 7-5 – Peak signals compared with response curve for a 4-in diameter shotput. ....	63

## Tables

Table 3-1 – Performance Objectives for the APG Demonstration .....	12
Table 3-2 – Performance Objectives for the former Camp SLO Demonstration .....	17
Table 4-1 – Geodetic Control at the APG Demonstration Site.....	24
Table 4-2 – Geodetic Control at the former Camp San Luis Obispo Demonstration Site.....	28
Table 6-1 – Partial prioritized dig list for the former Camp SLO TEMTADS demonstration.....	49
Table 7-1 – Performance Results for the APG Demonstration.....	51
Table 7-2 – TEMTADS Blind Grid Test Area $P_d^{disc}$ Results.....	52
Table 7-3 – TEMTADS Blind Grid Test Area $P_{fp}^{disc}$ Results.....	52
Table 7-4 – TEMTADS Indirect Fire Test Area $P_d^{disc}$ Results .....	53
Table 7-5 – TEMTADS Indirect Fire Test Area $P_{fp}^{disc}$ Results .....	53
Table 7-6 – TEMTADS Blind Grid Test Area Efficiency and Rejection Rates.....	54
Table 7-7 – TEMTADS Indirect Fire Test Area Efficiency and Rejection Rates .....	54
Table 7-8 – TEMTADS Blind Grid Test Area Location Error and Standard Deviation.....	55
Table 7-9 – TEMTADS Indirect Fire Test Area Location Error and Standard Deviation .....	55
Table 7-10 – Performance Objectives for the former Camp SLO Demonstration .....	58
Table 7-11 – Details of former Camp SLO Calibration Strip.....	59
Table 7-12 – Peak Signals for former Camp SLO Calibration Strip Emplaced Items .....	61
Table 7-13 – Position Accuracy and Variability for former Camp SLO Calibration Strip Emplaced Items.....	64
Table 8-1 – Summary of Costs for a 25-acre, 3000 anomaly TEMTADS survey.....	69



## Acronyms

AOL	Advanced Ordnance Locator
APG	Aberdeen Proving Ground
ATC	Aberdeen Test Center
DAQ	Data Acquisition Computer
DAS	Data Analysis System
EMI	Electromagnetic Induction
GIS	Geographic Information System
GPS	Global Positioning System
MTADS	Multi-sensor Towed Array Detection System
NMEA	National Marine Electronics Association
NRL	Naval Research Laboratory
POC	Point of Contact
(PTNL,)AVR	Time, Yaw, Tilt Range NMEA-0183 sentence
(PTNL,)GGK	Time, Position, Fix Quality, PDOP NMEA-0183 sentence
RTK	Real-time Kinematic
Rx	Receive
SNR	Signal-to-Noise Ratio
TEM	Time-domain Electromagnetic induction
TEMTADS	Time-domain Electromagnetic induction Towed Array Detection System
Tx	Transmit
UTC	Universal Time Coordinated
UXO	Unexploded Ordnance

## **ACKNOWLEDGEMENTS**

This project was a collaborative effort between the Naval Research Laboratory, Science Applications International Corporation (SAIC), and G&G Sciences. Dave George of G&G Sciences was responsible for the development of the EMI sensor technology on which the TEMTADS array was built. Tom Bell of SAIC and Dan Steinhurst and Glenn Harbaugh of Nova Research, Inc. collaborated on the design of the integrated TEMTADS array, the deployment of system. Jim Kingdon, Bruce Barrow, and Dean Keiswetter of SAIC were also involved in the modeling/analysis of the resultant data.

## EXECUTIVE SUMMARY

The technology focus of this demonstration is a vehicle-towed array of time-domain electromagnetic sensors designed and operated to optimize the classification of buried munitions from ancillary metallic debris and clutter. The demonstrated technology, known as the TEMTADS array, consists of 25 co-located transmit (Tx) and receive (Rx) pairs arranged in a 5x5 fixed grid configuration. The TxRx pairs are separated by 40cm center-to-center, which results in a 2m square array. Transient decay data are collected for each Rx coil with a 500 kHz sample rate until 25ms after turn off of the excitation pulse. The 25 Tx coils are operated individually while recording with all 25 Rx, resulting in 625 spatial measurements. The system is designed to interrogate subsurface sources one at a time sequentially. It collects data while stationary.

The raw signature data from the TEMTADS array reflect details of the sensor/target geometry as well as inherent EMI response characteristics of the targets themselves. In order to separate out the intrinsic target response properties from sensor/target geometry effects the measured signature is inverted to estimate principal axis magnetic polarizabilities using a standard induced dipole response model.

The TEMTADS array was designed to combine the data quality advantages of a gridded survey with the coverage efficiencies of a vehicular system. The design goal of this system is to collect data equal, if not better, in quality to the best gridded surveys (the relative position and orientation of the sensors being known better than for gridded data) while prosecuting many more targets each field day.

The objective of this demonstration was to validate the discrimination technology through two blind tests. The first demonstration was conducted at the Aberdeen Proving Ground (APG) Standardized UXO Test Site. The second demonstration was conducted as part of the ESTCP UXO Classification Study at the former Camp San Luis Obispo. At each demonstration, the site had been blind seeded with a significant number of intact, inert UXO types to challenge UXO classification systems and methodologies.

The performance metrics used to monitor the success of the technology relate to production rate, accuracy of inverted features, analysis time, correct classification, and ease of use. As detailed in later sections, all performance objectives were successfully met. At the APG site, the system was able to interrogate over 150 targets per day. The inverted source locations were less than 10 cm in northing and easting from the ground truth locations. The analysis, which required roughly 15 minutes per target, resulted in a false alarm reduction by over 50% with 95% correct identification of munitions.

At the former Camp San Luis Obispo site, the system acquired data at over 125 anomalies per day. All data were checked for quality on site and at pace with data collection. The average error in location was less than 5cm in northing and easting and the average error in depth estimation was less than 5cm.

Qualitatively, the TEMTADS array was easy to use and proved to be a robust and reliable sensor platform.

The primary limitation of this technology relates to the size of the system and site access. The array is a 2-m square so fields where the vegetation or topography interferes with passage of a trailer that size will not be amenable to the use of the 5x5 array.

## **1.0 INTRODUCTION**

### **1.1 BACKGROUND**

Unexploded Ordnance (UXO) detection and remediation is a high priority triservice requirement. As the Defense Science Board recently wrote: “Today’s UXO cleanup problem is massive in scale with some 10 million acres of land involved. Estimated cleanup costs are uncertain but are clearly tens of billions of dollars. This cost is driven by the digging of holes in which no UXOs are present. The instruments used to detect UXOs (generally located underground) produce many false alarms, - i.e., detections from scrap metal or other foreign or natural objects - , for every detection of a real unexploded munition found.” [1]

There is general agreement that the best solution to the false alarm problem involves the use of EMI sensors which, in principle, allow the extraction of target shape parameters in addition to a size and depth estimate. We, and others, have fielded systems with either time-domain or frequency-domain EMI sensors with the goal of extracting reliable target shape parameters and, thus, improving the discrimination capability of our surveys. In practice, the discrimination ability of these sensors has been limited by signal-to-noise limitations. Three of the largest noise terms are inherent sensor noise, motion-induced noise, and sensor location uncertainty.

The three most successful demonstrations of EMI-based discrimination all involved cued detection with gridded collection of EMI data [2-4]. The success of the gridded data collections was due to the combination of minimal location uncertainty, no motion-induced noise, and sufficient SNR. The downside of the implementations previously demonstrated is that they were relatively slow and inefficient, especially on a large site. We have constructed an EMI sensor array that combines the classification ability of a gridded survey with the coverage efficiency of a vehicular array. By coming to a stop over each target to be investigated we are able to obtain all the benefits of a gridded survey (negligible relative sensor location uncertainty, no motion-induced noise, and high SNR) while moving rapidly to the next target with no set-up required gives us the coverage efficiency required for practical success.

### **1.2 OBJECTIVE OF THE DEMONSTRATION**

The objective of this demonstration was to validate the technology through a series of blind test demonstrations. We conducted a shake-down demonstration of the technology at our Blossom Point, MD field site but a blind test is the only true measure of system performance. The first demonstration was conducted at the Aberdeen Proving Ground (APG) Standardized UXO Test Site. The second demonstration was conducted as part of the ESTCP UXO Classification Study at the former Camp San Luis Obispo. At each demonstration, the site had been blind seeded with a significant number of intact, inert UXO types to challenge UXO classification systems and methodologies. Demonstration scoring was conducted by IDA to maintain the integrity of the ground truth.

## 1.3 REGULATORY DRIVERS

Stakeholder acceptance of the use of classification techniques on real sites will require demonstration that these techniques can be deployed efficiently and with high probability of discrimination. The first step in this process is to demonstrate acceptable performance on synthetic test sites such as that at Aberdeen. As a second step, demonstration on a carefully prepared and blind-seeded live site presents a more real-world scenario while providing sufficiently complete validation data to accurately determine system performance. After these hurdles have been passed, successful demonstration at a live site will further facilitate regulatory acceptance of the UXO classification technology and methodology.

## 2.0 TECHNOLOGY

### 2.1 TECHNOLOGY DESCRIPTION

#### 2.1.1 EMI Sensors

The EMI sensor used in the TEMTADS array is based on the Navy-funded Advanced Ordnance Locator (AOL), developed by G & G Sciences. The AOL consists of three transmit coils arranged in a 1-m cube; we have adopted the transmit (Tx) and receive (Rx) subsystems of this sensor directly, converted to a 5 x 5 array of 35 cm sensors, and made minor modifications to the control and data acquisition computer to make it compatible with our deployment scheme.

A photograph of an individual sensor element under construction is shown in the left panel of Figure 2-1. The transmit coil is wound around the outer portion of the form and is 35 cm on a side. The 25-cm receive coil is wound around the inner part of the form which is re-inserted into the outer portion. An assembled sensor with the top and bottom caps used to locate the sensor in the array is shown in the right panel of Figure 2-1.

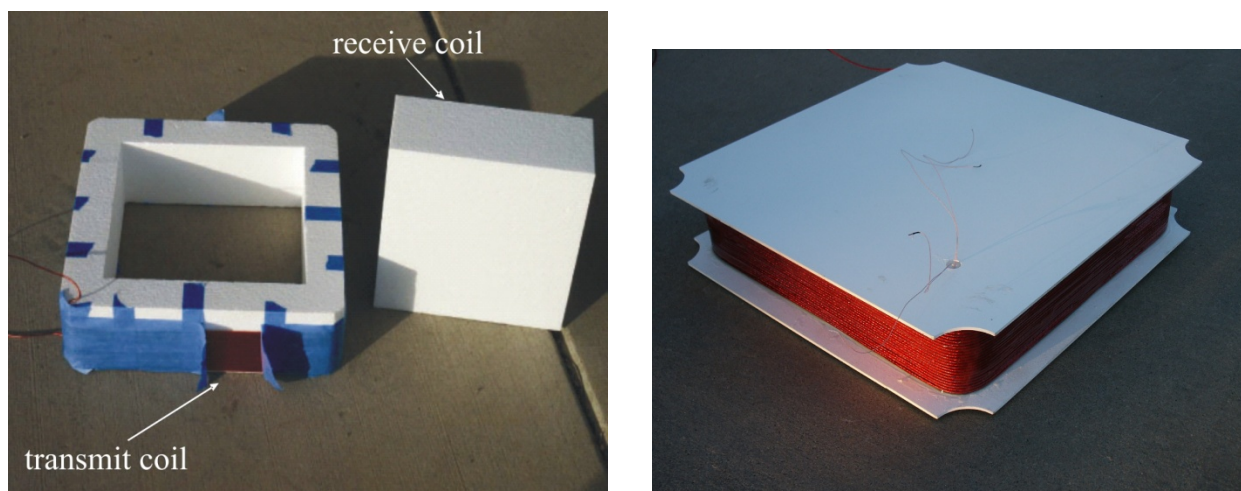


Figure 2-1 – Construction details of an individual EMI sensor (left panel) and the assembled sensor with end caps attached (right panel).

Decay data are collected with a 500 kHz sample rate until 25ms after turn off of the excitation pulse. This results in a raw decay of 12,500 points; too many to be practical. These raw decay measurements are grouped into 115 logarithmically-spaced “gates” whose center times range from 42  $\mu$ s to 24.35 ms with 5% widths and are saved to disk. Examples of the measured transmit pulse, raw decay, and gated decay are shown in Figure 2-2.

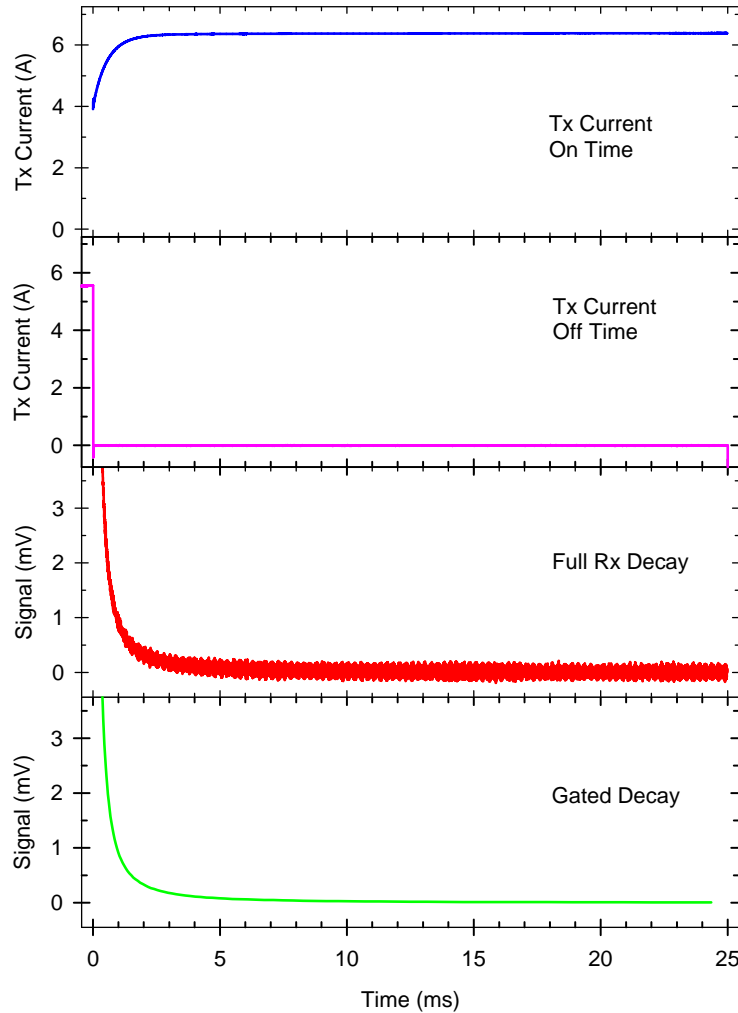


Figure 2-2 – Measured transmit current (on-time upper panel, off-time second panel), full measured signal decay (third panel), and gated decay (fourth panel) as discussed in the text.

### 2.1.2 Sensor Array

The twenty-five individual sensors are arranged in a 5 x 5 array as shown in Figure 2-3. The center-to-center distance is 40 cm yielding a 2 m x 2 m array. Also shown in Figure 2-3 is the

position of the three GPS antennae that are used to determine the location and orientation of the array for each cued measurement. A picture of the array mounted on the MTADS EMI sensor platform is shown in Figure 2-4.

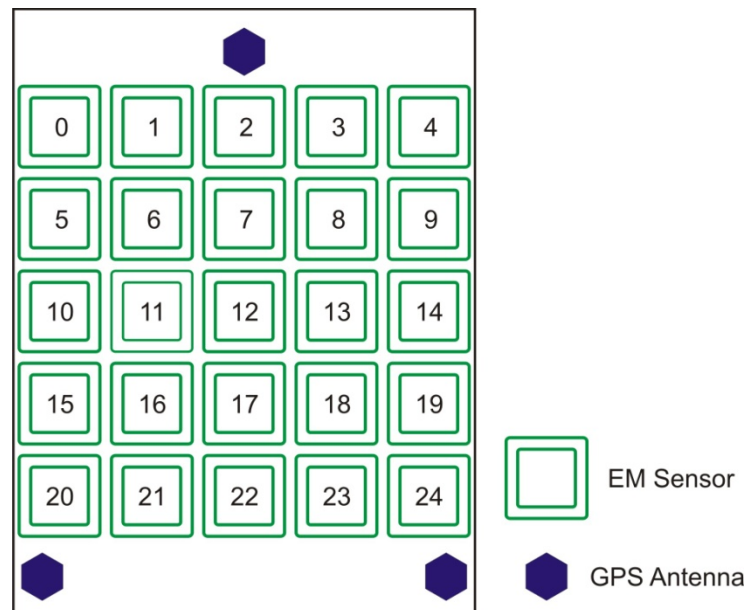


Figure 2-3 – Sketch of the EMI sensor array showing the position of the 25 sensors and the three GPS antennae.



Figure 2-4 – Sensor array mounted on the MTADS EMI sensor platform.

### **2.1.3 Application of the Technology**

Application of this technology is straightforward. A list of target positions is developed from a survey by some geophysical instrument; in the case of these demonstrations, either the MTADS magnetometer array at APG or the EM61 MkII array at SLO. This target file, containing the target location and an optional flag for additional ‘stacking’ or averaging, is transferred to the system control program which uses the information from the three GPS antennae to guide the operator to position the array over each target in turn. When positioned over the target, the data acquisition computer steps through the array sensors sequentially, just as in the characterization measurements discussed in the following section, and collects decays from all twenty-five receive coils for each excitation. These data are then inverted for target location and characteristics. At the end of the EMI data collection, a few seconds of platform position and orientation data are collected to be used to translate the inverted target position, which is, of course, relative to the array, to absolute position and orientation.

In the final version of this technology, one could envision the inversion being performed while the operator is driving the array to the next target. For these demonstrations, we performed the inversions off-line so that we would have the ability to intervene in the automatic process as required. The EMI and position data were transferred to the analyst several times each day for near real-time analysis at the demonstration site.

## **2.2 TECHNOLOGY DEVELOPMENT**

The individual sensors (consisting of transmit electronics, transmit and receive coils, pre-amp, and digitizer) were characterized at G & G Sciences before approval was given for construction of the array. Examples of the characterization data are shown in Figure 2-5 and Figure 2-6. System stability is shown in Figure 2-5 which plots the normalized (by measured transmit current) response of a 2 in steel ball at 25 cm separation from the sensor. The data plotted are decays 1, 1001, 2001, and 3001 in a continuously-triggered series that began from a cold start and ran for 150 minutes.

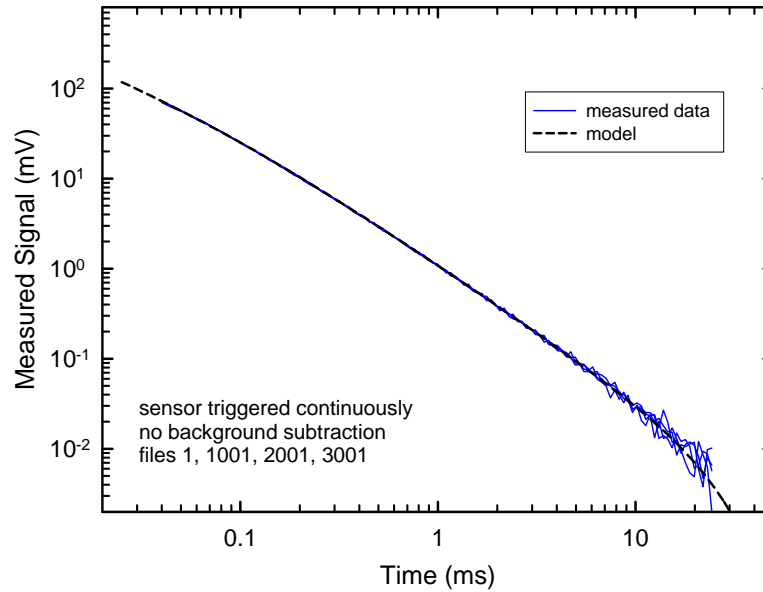


Figure 2-5 – Measured response from a 2-in steel sphere 25 cm from the sensor. Decays 1, 1001, 2001, and 3001 from a series that started from a cold start are plotted along with the expected response from this target.

For comparison purposes, the expected response from this sphere is plotted in black. As can be seen, the sensor exhibits excellent stability which is important for cued deployment.

The second important characterization test is sensor response linearity. Since we collect decay data to late times and over several orders of magnitude in amplitude, the linearity of system response is very important. To characterize this property of the sensor, we constructed a series of copper coils with nominal decay time constants of 2, 4, and 6 ms. The response of the three coils is shown in Figure 2-6 which plots the measured decay on semi-log axes. After a transient at early times, the decays exhibit clean exponential behavior with measured decay times of 1.8, 3.3, and 5.8 ms. Careful calculation of the expected decay times at the temperature at which the tests were conducted results in expected values of 1.82, 3.26, and 5.73 ms; the measured values are in excellent agreement with these.

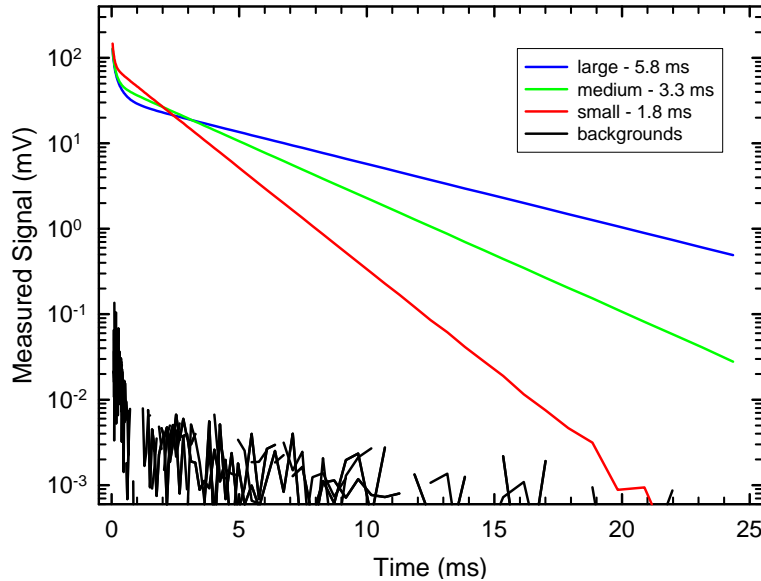


Figure 2-6 – Measured response from three calibration coils and the background response between measurements plotted on a semi-log plot to emphasize the exponential nature of the decay. The decay time constants extracted from the measurements are listed in the legend.

After assembly of the array, a number of array calibration measurements were performed. The first task was to ensure that each of the individual sensors has equivalent response. A jig was constructed that allowed us to mount a 2-in steel sphere 30 cm below each array element in turn. Data collected using this jig are shown in Figure 2-7. As can be seen, the measured decays from each of the sensors plotted are indistinguishable.

The assembled array was then used to measure the response of a number of inert ordnance items and stimulants mounted on a test stand, placed in our test pit, or buried in our test field. For each series of measurements with the full array, we cycle through the sensors transmitting from each in turn. After each excitation pulse, we record the response of all twenty-five receive coils. Thus, there are 625 (25 x 25) individual transmit/receive pairs recorded, making it difficult to present a full measurement in any coherent way. In Figure 2-8, we plot nine of the transmit/receive pairs resulting from excitation of a 40-mm projectile located under the center of the array. The decays plotted correspond to the signal received on the nine central sensors (reference Figure 2-3 for the sensor numbering) when that sensor transmits. In other words, the results of nine individual monostatic measurements are presented.

All 625 measurements are used for the inversion to recover target parameters. The inversion results for the decay data shown in Figure 2-8 are shown in Figure 2-9. As we expect for an object with axial symmetry such as a 40-mm projectile, we recover one large response coefficient and two equal, but smaller ones. These response coefficients are the basis of the discrimination decisions in this demonstration. Derived  $\beta$ s for “Cylinder E” (3" x 12" steel cylinder) in the test field are shown for comparison in Figure 2-10.

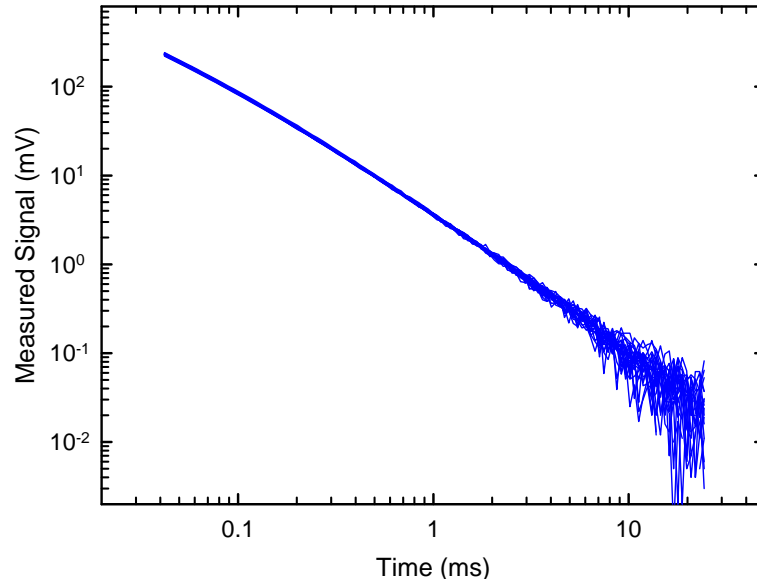


Figure 2-7 – Comparison of the response of the array members. The measured decay from a 2-in steel sphere held 30 cm below each sensor in turn is plotted. The decays are indistinguishable.

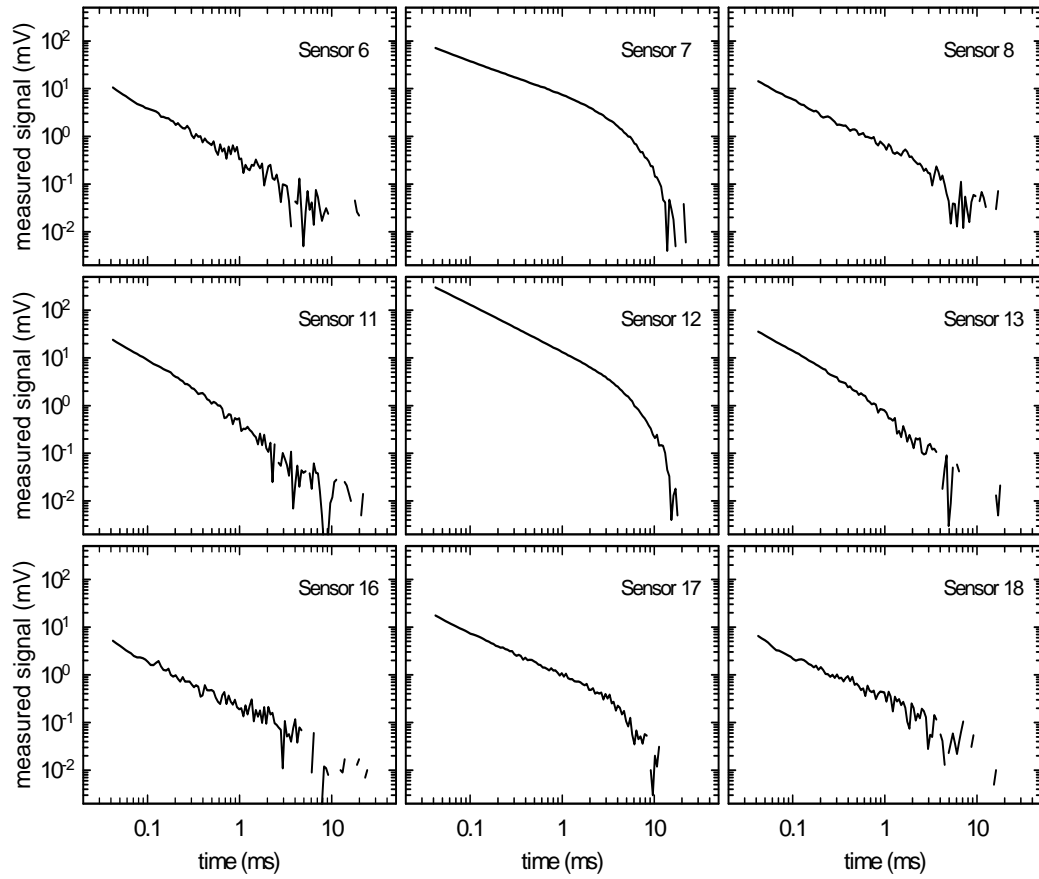


Figure 2-8 – The response of nine of the individual sensors to a 40-mm projectile located under the center of the array.

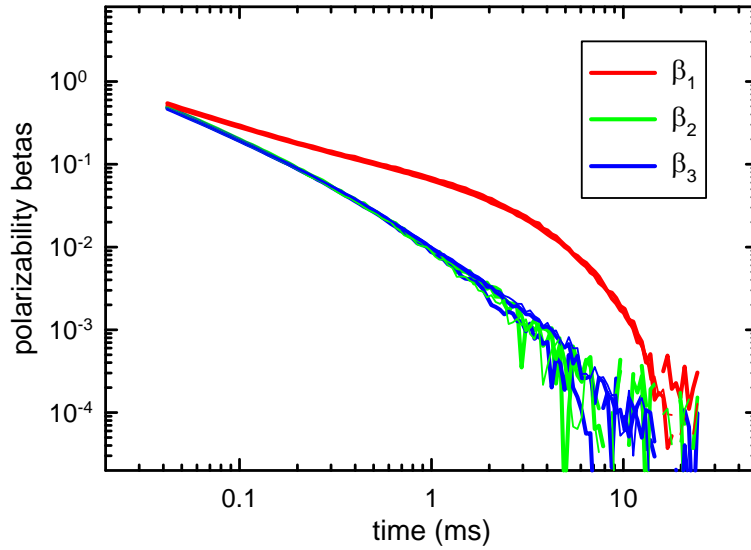


Figure 2-9 – Derived response coefficients for a 40-mm projectile using the measurements of which the decays shown in Figure 2-8 are a subset.

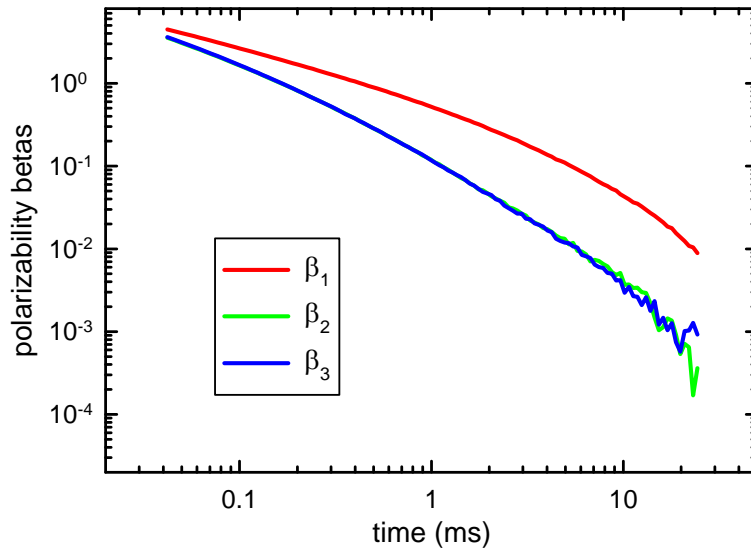


Figure 2-10 – Derived response coefficients from a cued measurement over "Cylinder E" in the test field.

The final array characterization test was to confirm that the response coefficients we recover are invariant to object position and orientation under the array. Figure 2-11 shows the derived  $\beta$ s plotted for a 4.2-in mortar baseplate after measurements at three position/orientation pairs. As can be seen, the inversion results are robust to variation in the object's position and orientation.

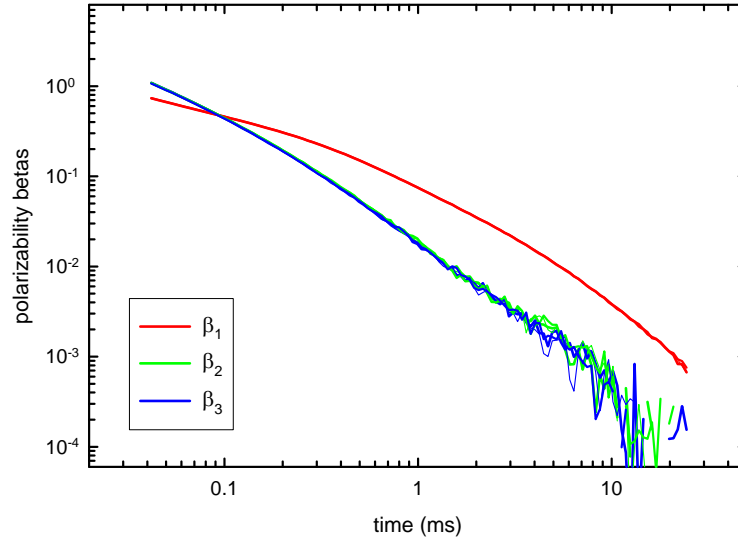


Figure 2-11 – Three sets of  $\beta$ s derived from three measurements over a 4.2-in mortar baseplate at different position/orientation pairs.

### 2.3 ADVANTAGES AND LIMITATIONS OF THE TECHNOLOGY

The TEMTADS array is designed to combine the data quality advantages of a gridded survey with the coverage efficiencies of a vehicular system. The design goal of this system is to collect data equal, if not better, in quality to the best gridded surveys (the relative position and orientation of the sensors being known better than for gridded data) while prosecuting many more targets each field day.

There are obvious limitations to the use of this technology. The array is a 2-m square so fields where the vegetation or topography interferes with passage of a trailer that size will not be amenable to the use of the present array. The other serious limitation will be anomaly density. For all sensors, there is a limiting anomaly density above which the response of individual targets cannot be separated. We have chosen relatively small sensors for this array which should help with this problem but we cannot eliminate it. Based on experiments at our test pit at Blossom Point, the results of this demonstration, and work done on the former Camp Sibert data sets, anomaly densities of 300 anomalies/acre or higher would limit the applicability of this system as more than 20% of the anomalies would have another anomaly within a meter. For low SNR targets, our standard data acquisition parameters may not be sufficient. The system software has built in the capability to vary the data acquisition parameters on-the-fly based on flags in the target file and can be reconfigured manually as required. One area in need of development is a robust, consolidated data collection / data QC methodology for determining when there is a low SNR anomaly and when there is no anomaly present. This issue is an area of ongoing research.

### 3.0 PERFORMANCE OBJECTIVES

The TEMTADS array was deployed to demonstrations at both the APG Standardized UXO Test Site and the ESTCP UXO Classification Study site at the former Camp SLO. The performance objectives for these demonstrations are summarized in Table 3-1. Since the TEMTADS array is a discrimination technology, the performance objectives focus on the second step of the UXO survey problem; we assume that the anomalies from all targets of interest have been detected and included on the target list that we worked from.

Due to the nature of the demonstrations at each site and the employed scoring methods, separate Performance Objectives are provided for each demonstration in the following subsections.

#### 3.1 APG STANDARDIZED UXO TEST SITE

Table 3-1 – Performance Objectives for the APG Demonstration

Performance Objective	Metric	Data Required	Success Criteria	Results
Reduction of False Alarms	Number of false alarms eliminated at demonstrator operating point.	<ul style="list-style-type: none"><li>• Prioritized dig list</li><li>• Scoring report from APG</li></ul>	Reduction of false alarms by > 50% with 95% correct identification of munitions	Yes
Location Accuracy	Average error and standard deviation in both axes for interrogated items	<ul style="list-style-type: none"><li>• Estimated location from analysis</li><li>• Scoring report from APG</li></ul>	$\Delta N$ and $\Delta E < 10$ cm $\sigma N$ and $\sigma E < 15$ cm	Yes
Production Rate	Number of targets interrogated each day	<ul style="list-style-type: none"><li>• Log of field work</li></ul>	75 targets per day	Yes
Analysis Time	Average time required for inversion and classification	<ul style="list-style-type: none"><li>• Log of analysis work</li></ul>	15 min per target	Yes
Ease of Use		<ul style="list-style-type: none"><li>• Feedback from operator on ease of use</li></ul>	Operator comes to work smiling	Yes

### **3.1.1 OBJECTIVE: REDUCTION OF FALSE ALARMS**

This is the primary measure of the effectiveness of this technology. By collecting high-quality, precisely-located data, we expect to be able to discriminate munitions from scrap and frag with high efficiency.

#### **3.1.1.1.Metric**

At a seeded test site such as the APG standardized test site, the metric for false alarm elimination is straightforward. We prepared a ranked dig list for the targets we interrogated with a dig/no-dig threshold indicated and ATC personnel used their automated scoring algorithms to assess our results.

#### **3.1.1.2.Data Requirements**

The identification of most of the items in the test field is known to the test site operators. Our ranked dig list is the input for this standard and ATC's standard scoring is the output.

#### **3.1.1.3.Success Criteria**

The objective will be considered to be met if more than 50% of the non-munitions items were labeled as no-dig while retaining 95% of the munitions items on the dig list.

#### **3.1.1.4.Results**

This Objective was successfully met. The TEMTADS surveyed anomalies detected by the MTADS magnetometer system in the Blind Grid and Indirect Fire Areas. Efficiency (E) and false positive rejection rate ( $R_{fp}$ ) are used to score discrimination performance ability at two specific operating points on a ROC curve: one at the point where no decrease in  $P_d$  is incurred and the other at the operator-selected threshold. Efficiency is defined as the fraction of detected ordnance correctly classified as ordnance and the false positive rejection rate is defined as the fraction of detected clutter correctly classified as clutter. The results for the Blind Grid and Indirect Fire Test Areas were  $E = 0.99$  and  $R_{fp} = 0.99$ , and  $E = 0.98$  and  $R_{fp} = 0.92$  at the operating point, respectively. With no loss of  $P_d$ , the results were  $E = 1.00$  and  $R_{fp} = 0.95$ , and  $E = 1.00$  and  $R_{fp} = 0.58$ , for the Blind Grid and the Indirect Fire Areas respectively. These data are summarized from Tables 7a and 7c of Reference 15.

### **3.1.2 OBJECTIVE: LOCATION ACCURACY**

An important measure of how efficiently any required remediation will proceed is the accuracy of predicted location of the targets marked to be dug. Large location errors lead to confusion among the UXO techs assigned to the remediation costing time and often leading to removal of a small, shallow object when a larger, deeper object was the intended target.

#### **3.1.2.1.Metric**

As above, the metric for location accuracy is straightforward at a seeded test site such as the APG standardized test site. We provided an estimated position for all targets we interrogated and ATC personnel used their automated scoring algorithms to assess our results.

#### **3.1.2.2.Data Requirements**

The location of most of the items in the test field is known to the test site operators. Our dig list is the input for this standard and ATC's standard scoring is the output.

#### **3.1.2.3.Success Criteria**

The objective will be considered to be met if the average position error was less than 10 cm in both dimensions (low bias) and the standard deviation of each dimension was less than 15 cm (accurate location).

#### **3.1.2.4.Results**

This Objective was successfully met. The location accuracy of fit parameters generated from the TEMTADS array data, taken from Tables 9a and 9c of Reference 15, are within 5 cm horizontally ( $1\sigma$ ) and 6 cm vertically ( $1\sigma$ ) for the Indirect Fire Area. Horizontal errors are not calculated for the Blind Grid. The vertical accuracy was 4 cm ( $1\sigma$ ) for the Blind Grid.

### **3.1.3 OBJECTIVE: PRODUCTION RATE**

Even if the performance of the technology on the two metrics above is satisfactory, there is an economic metric to consider. There is a known cost of remediating a suspected munitions item. If the cost to interrogate a target is greater than this cost, the technology will be useful only at sites with special conditions or target values. Note, however, that in its ultimate implementation this technology will result in reacquisition, cued interrogation, and target flagging in one visit to the site.

#### **3.1.3.1.Metric**

The number of targets interrogated per day is the metric for this objective. Combined with the daily operating cost of the technology this gives the per-item cost.

#### **3.1.3.2.Data Requirements**

Survey productivity was determined from a review of the ATC demonstration field logs.

#### **3.1.3.3.Success Criteria**

For this first demonstration, the objective will be considered to be met if at least 75 targets were interrogated each survey day.

#### **3.1.3.4.Results**

This Objective was successfully met. Data collection times are taken from Table 5 of Reference 15. 214 anomalies were investigated on the Blind Grid over the course of 1.43 work days, or on average 149 anomalies / work day. 694 anomalies were investigated in the Indirect Fire Area over the course of 32 hours and 30 minutes, or on average 170 anomalies / work day.

#### **3.1.4 OBJECTIVE: ANALYSIS TIME**

The ultimate implementation of this technology will involve on-the-fly analysis and classification. The time for this will be limited to the driving time to the next anomaly on the list. We will track the near-real-time analysis time in this demonstration.

##### **3.1.4.1.Metric**

The time required for inversion and classification per anomaly is the metric for this objective

##### **3.1.4.2.Data Requirements**

Analysis time was determined from a review of the data analysis logs.

##### **3.1.4.3.Success Criteria**

For this first demonstration, the objective will be considered to be met if the average inversion and classification time was less than 15 min.

##### **3.1.4.4.Results**

This Objective was successfully met. The average inversion time per target was approximately 2.5 minutes on our field laptop computer. Including this, the average analysis time amounted to 12.5 minutes per anomaly. Since this was the first extensive test of the system in field mode, we took the opportunity to consider various discrimination and classification methods, some of which proved unfruitful. As a result of lessons learned from this undertaking, we expect the average analysis time for future field runs to be less than that obtained here.

#### **3.1.5 OBJECTIVE: EASE OF USE**

This qualitative objective is intended as a measure of the long-term usability of the technology. If the operator does not report that the technology is easy to use, shortcuts that can compromise the efficiency of the technology will begin to creep into daily operations.

##### **3.1.5.1.Data Requirements**

This objective was evaluated based on operator feedback.

### **3.1.5.2.Results**

This Objective was successfully met. Based on vehicle operator feedback, there were no significant limitations to the efficient use of the system in the field. Several suggestions were made for additional improvements to the navigation and data collection software. They have been subsequently incorporated. Based on the suggestions, anomalies for future demonstrations will be ordered along 1m swaths for maximum data collection efficiency.

## 3.2 FORMER CAMP SAN LUIS OBISPO

Table 3-2 – Performance Objectives for the former Camp SLO Demonstration

Performance Objective	Metric	Data Required	Success Criteria	Results
<b>Quantitative Performance Objectives</b>				
Site Coverage	Fraction of assigned anomalies interrogated	Survey results	100% as allowed for by topography / vegetation	Yes
Calibration Strip Results	System response consistently matches physics-based model	System response curves Daily calibration strip data	$\leq 15\%$ rms variation in amplitude Down-track location $\pm 25\text{cm}$ All response values fall within bounding curves	No
Location Accuracy	Average error and standard deviation in both axes for interrogated items	Estimated location from analyses Ground truth from validation effort	$\Delta N$ and $\Delta E < 5\text{ cm}$ $\sigma N$ and $\sigma E < 10\text{ cm}$	No
Depth Accuracy	Standard deviation in depth for interrogated items	Estimated location from analyses Ground truth from validation effort	$\Delta \text{Depth} < 5\text{ cm}$ $\sigma \text{Depth} < 10\text{ cm}$	No
Production Rate	Number of anomalies investigated each day	Survey results Log of field work	125 anomalies/day	Yes
Data Throughput	Throughput of data QC process	Log of analysis work	All data QC'ed on site and at pace with survey	Yes
<b>Qualitative Performance Objective</b>				
Reliability and Robustness	General Observations	Team feedback and recording of emergent problems	Field team comes to work smiling	Yes

### 3.2.1 OBJECTIVE: SITE COVERAGE

A list of previously identified anomalies will be provided by the Program Office. The expectation is to gather cued data with the TEMTADS system over each anomaly.

#### **3.2.1.1.Metric**

Site coverage is defined as the fraction of the assigned anomalies surveyed by the TEMTADS. Exceptions are to be made for topology / vegetation interferences.

#### **3.2.1.2.Data Requirements**

The collected data will be compared to the original anomaly list. Any interferences will be noted in the field log book as they occur.

#### **3.2.1.3.Success Criteria**

The objective will be considered met if 100% of the assigned anomalies are surveyed with the exception of areas that can not be surveyed due to topology / vegetation interferences.

#### **3.2.1.4.Results**

This objective was successfully met. Of the list provided by the Program Office, all but 5 were measured. Failure to measure these 5 anomalies was due to the presence of rocks which prevented the operator from positioning the TEMTADS over the target.

### **3.2.2 OBJECTIVE: CALIBRATION STRIP RESULTS**

This objective supports that each sensor system is in good working order and collecting physically valid data each day. The calibration strip is to be surveyed twice daily. The peak positive response of each emplaced item from each run is compared to the physics-based response curves generated prior to data collection on site using each item of interest.

#### **3.2.2.1.Metric**

The reproducibility of the measured response of each sensor system to the items of interest and the comparison of the response to the response predicted by the physics-based model defines this metric.

#### **3.2.2.2.Data Requirements**

Response curves for each sensor / item of interest pair are used to document what the physics-based response of the system to the item should be. The tabulated peak response values from each survey of the Calibration Strip demonstrates the reproducibility and validity of the sensor readings.

#### **3.2.2.3.Success Criteria**

The objective will be considered met if all measured responses fall within the range of physically possible values based on the appropriate response curve. Additionally, the RMS variation in

responses should be less than 15% of the measured response and the down-track location of the anomaly should be within 25 cm of the corresponding seeded item's true location.

#### **3.2.2.4.Results**

This objective was not successfully met in full. The measured peak signals for all of the emplaced items are shown in Figure 7-1 thru Figure 7-4. The maximum (red) and minimum (blue) response curves are plotted for all objects except the shotput, which has only one curve due to symmetry. The two curves for the 81-mm and 4.2-in mortar are nearly equal. For self-consistency, we have plotted the measurements at the mean inverted depth, rather than the reported depths. The measured values generally fit well within the bounding curves, with the 4.2-in mortar and shotput results the poorest, with a tendency to underestimate the peak value.

Careful examination of the data shows that this variation is the result of the shot-to-shot precision with which the array can be positioned in exactly the same spot each time. Because the response curves are generated assuming the target is directly below the sensor, any offset in the sensor position will result in the derived peak signal being smaller than that predicted by the curve, as is observed. For future demonstrations, the metric of polarizability amplitude is recommended as these values are invariant to array position.

### **3.2.3 OBJECTIVE: LOCATION ACCURACY**

An important measure of how efficiently any required remediation will proceed is the accuracy of predicted location of the targets marked to be dug. Large location errors lead to confusion among the UXO technicians assigned to the remediation costing time and often leading to removal of a small, shallow object when a larger, deeper object was the intended target.

#### **3.2.3.1.Metric**

The average error and standard deviation in both horizontal axes will be computed for the items which are selected for excavation during the validation phase of the study.

#### **3.2.3.2.Data Requirements**

The anomaly fit parameters and the ground truth for the excavated items will be required to determine the performance of the fitting routines in terms of the location accuracy.

#### **3.2.3.3.Success Criteria**

This objective will be considered as met if the average error in position for both Easting and Northing quantities is less than 5 cm and the standard deviation for both is less than 10 cm.

#### **3.2.3.4.Results**

This objective was not successfully met in full. The average Northing position error for all measured data was 1.5cm, while the average Easting position error was 3cm. The standard

deviations, however, were larger than desired, with both values about 25cm. Excluding those anomalies for which multiple targets were found produces negligible improvement. We suspect the higher values are due to the large number of small, low SNR clutter items, which result in greater uncertainty in both the measured and fitted values. Indeed, if we restrict ourselves to those anomalies which we classified as likely UXO, the Northing and Easting standard deviations drop to 7cm and 5cm, respectively.

### **3.2.4 OBJECTIVE: DEPTH ACCURACY**

An important measure of how efficiently any required remediation will proceed is the accuracy of predicted depth of the targets marked to be dug. Large depth errors lead to confusion among the UXO technicians assigned to the remediation costing time and often leading to removal of a small, shallow object when a larger, deeper object was the intended target.

#### **3.2.4.1.Metric**

The standard deviation of the predicted depths with respect to the ground truth will be computed for the items which are selected for excavation during the validation phase of the study.

#### **3.2.4.2.Data Requirements**

The anomaly fit parameters and the ground truth for the excavated items will be required to determine the performance of the fitting routines in terms of the predicted depth accuracy.

#### **3.2.4.3.Success Criteria**

This objective will be considered as met if the average error in depth is less than 5 cm and the standard deviation is less than 10 cm.

#### **3.2.4.4.Results**

This objective was not met successfully in full. The average depth error for all measured data was 2.5cm. The standard deviation was a bit larger than desired, with a value of 14cm. Excluding those anomalies for which multiple targets were found and restricting the analysis to those anomalies classified as ‘likely UXO’ to exclude low SNR clutter items, the standard deviation drops to 7cm.

### **3.2.5 OBJECTIVE: PRODUCTION RATE**

This objective considers a major cost driver for the collection of high-density, high-quality geophysical data, the production rate. The faster quality data can be collected, the higher the financial return on the data collection effort.

#### **3.2.5.1.Metric**

The number of anomalies investigated per day determines the production rate for a cued survey system.

#### **3.2.5.2.Data Requirements**

The metric can be determined from the combination of the field logs and the survey results. The field logs record the amount of time per day spent acquiring the data and the survey results determine the number of anomalies investigated in that time period.

#### **3.2.5.3.Success Criteria**

This objective will be considered met if average production rate is at least 125 anomalies / day.

#### **3.2.5.4.Results**

This objective was successfully met. A total of 1547 anomalies (including redo's) were measured over a 10-day run for an average of 155 anomalies/day. The only days for which our average fell below our goal of 125 anomalies/day were the final day, due to finishing up all targets, and 2 days in which necessary vehicle repairs shortened our workday.

### **3.2.6 OBJECTIVE: DATA THROUGHPUT**

The collection of a complete, high-quality data set with the sensor platform is critical to the downstream success of the UXO Classification Study. This objective considers one of the key data quality issues, the ability of the data analysis workflow to support the data collection effort in a timely fashion. To maximize the efficient collection of high quality data, a series of MTADS standard data quality check are conducted during and immediately after data collection on site. Data which pass the QC screen are then processed into archival data stores. Individual anomaly analyses are then conducted on those archival data stores. The data QC / preprocessing portion of the workflow needs to keep pace with the data collection effort for best performance.

#### **3.2.6.1.Metric**

The throughput of the data quality control workflow is at least as fast the data collection process, providing real time feedback to the data collection team of any issues.

#### **3.2.6.2.Data Requirements**

The data analysts log books will provide the necessary data for determining the success of this metric.

### **3.2.6.3.Success Criteria**

This objective will be considered met if all collected data can be processed through the data quality control portion of the workflow in a timely fashion.

### **3.2.6.4.Results**

This objective was successfully met. Data were normally downloaded several times during each workday, and quality control on these datasets was usually completed on the same day. Quality control checks successfully caught missed anomalies, a small number of corrupt data files, and targets which needed re-measuring.

For low SNR targets, our standard data acquisition parameters may not be sufficient. The system software has built in the capability to vary the data acquisition parameters on-the-fly based on flags in the target file and can be reconfigured manual as required. To date these capabilities have not been demonstrated and could potentially have an impact on data throughput. A robust, consolidated data collection / data QC methodology for determining when there is a low SNR anomaly and when there is no anomaly present is necessary to accurately and efficiently utilize these capabilities. This issue is an area of ongoing research.

## **3.2.7 OBJECTIVE: RELIABILITY AND ROBUSTNESS**

This objective represents an opportunity for all parties involved in the data collection process, especially the vehicle operator, to provide feedback on areas where the process could be improved.

### **3.2.7.1.Data Requirements**

Discussions with the entire field team and other observations will be used.

### **3.2.7.2.Results**

This objective was successfully met. Based on vehicle operator feedback, there were no significant limitations to the efficient use of the system in the field.

## **4.0 SITE DESCRIPTION**

Two demonstrations were conducted for this project. The first was conducted at the APG Standardized UXO Technology Demonstration Site located at the Aberdeen Proving Ground, MD during the period of May through June, 2008. The second was conducted at the former Camp San Luis Obispo, CA ESTCP UXO Classification Study Demonstration Site in June, 2009.

## **4.1 APG STANDARDIZED UXO TECHNOLOGY DEMONSTRATION SITE**

### **4.1.1 SITE SELECTION**

This was our first field demonstration of this combination of EMI sensors and survey mode. As such, the demonstration was conducted on the Standardized UXO Test Site at APG. The APG site is located close to our base of operations in southern Maryland and therefore minimizes the logistics costs of the deployment. Use of this site allows us to receive validation results from near-real-world conditions without incurring the logistics and intrusive investigation expenses that would be required for a demonstration at a live site.

### **4.1.2 SITE HISTORY**

The Standardized UXO Technology Demonstration Site is adjacent to the Trench Warfare facility at the Aberdeen Proving Ground. The specific area was used for a variety of ordnance tests over the years. Initial magnetometer and EMI surveys conducted by the MTADS team performed after a “mag and flag” survey of the same area identified over a thousand remaining anomalies. These data were used for a final clean up of the site prior to the emplacement of the original test items. Prior to the two subsequent reconfiguration events, unexplained anomalies identified by demonstrators using the site were also investigated and removed.

### **4.1.3 SITE TOPOGRAPHY AND GEOLOGY**

According to the soils survey conducted for the entire area of APG in 1998, the test site consists primarily of Elkton Series type soil [5]. The Elkton Series consist of very deep, slowly permeable, poorly drained soils. These soils formed in silty aeolin sediments and the underlying loamy alluvial and marine sediments. They are on upland and lowland flats and in depressions of the Mid-Atlantic Coastal Plain. Slopes range from 0 to 2 percent.

Overall, the demonstration site is relatively flat and level. There are some low-lying areas in the northwest portion of the site that tend to have standing water during the wet periods of the year. The current sensor system is not sufficiently weatherproofed to operate through standing water. However, during the most recent reconfiguration, the areas most prone to being underwater were excluded from the survey scenarios. Anomalies that were located underwater or nearby to water at the time of survey were deferred until the end of the survey and were interrogated by carefully, if less efficiently, maneuvering the array into position.

### **4.1.4 MUNITIONS CONTAMINATION**

The area currently occupied by the Standardized site has seen an extensive history of munitions use. As an example, in 2003 we conducted a magnetometer survey of a previously unremediated area directly adjacent to the Standardized site [6]. In a survey area of approximately 1 hectare, we identified 2479 anomalies, of which 1921 were amenable to a model fit using our standard analysis. Historical records provided by ATC and previous remediation results indicated that the likely munitions of interest for this site were:

- Grenades, MkI, MkII, and French VB Rifle w/o chute
- Grenades, French VB Rifle w/ chute
- 60mm mortars (including 2" Smoke)
- 3" Stokes (Smoke and HE)
- 105 mm projectiles
- 155 mm projectiles

#### 4.1.5 SITE GEODETIC CONTROL INFORMATION

There are two first-order points on the site for use as GPS base station points. Their reported coordinates are listed in Table 4-1. The horizontal datum for all values is NAD83. The vertical control is referenced to the NAVD88 datum and the Geoid03 geoid. Point 477 was used as the GPS base station point for the entirety of this demonstration.

Table 4-1 – Geodetic Control at the APG Demonstration Site

ID	Latitude	Longitude	Elevation	Northing	Easting	HAE
477	39° 28' 18.63880" N	76° 07' 47.71815"W	10.669 m	4,369,749.013	402,810.038	-22.545
478	39° 28' 04.24219" N	76° 07' 48.50439"W	11.747 m	4,369,305.416	402,785.686	-21.473

#### 4.1.6 SITE CONFIGURATION

Figure 4-1 is a map of the Standardized UXO Technology Demonstration Site at APG. The Calibration and Blind Grids are shown along with the various Open Field Areas.

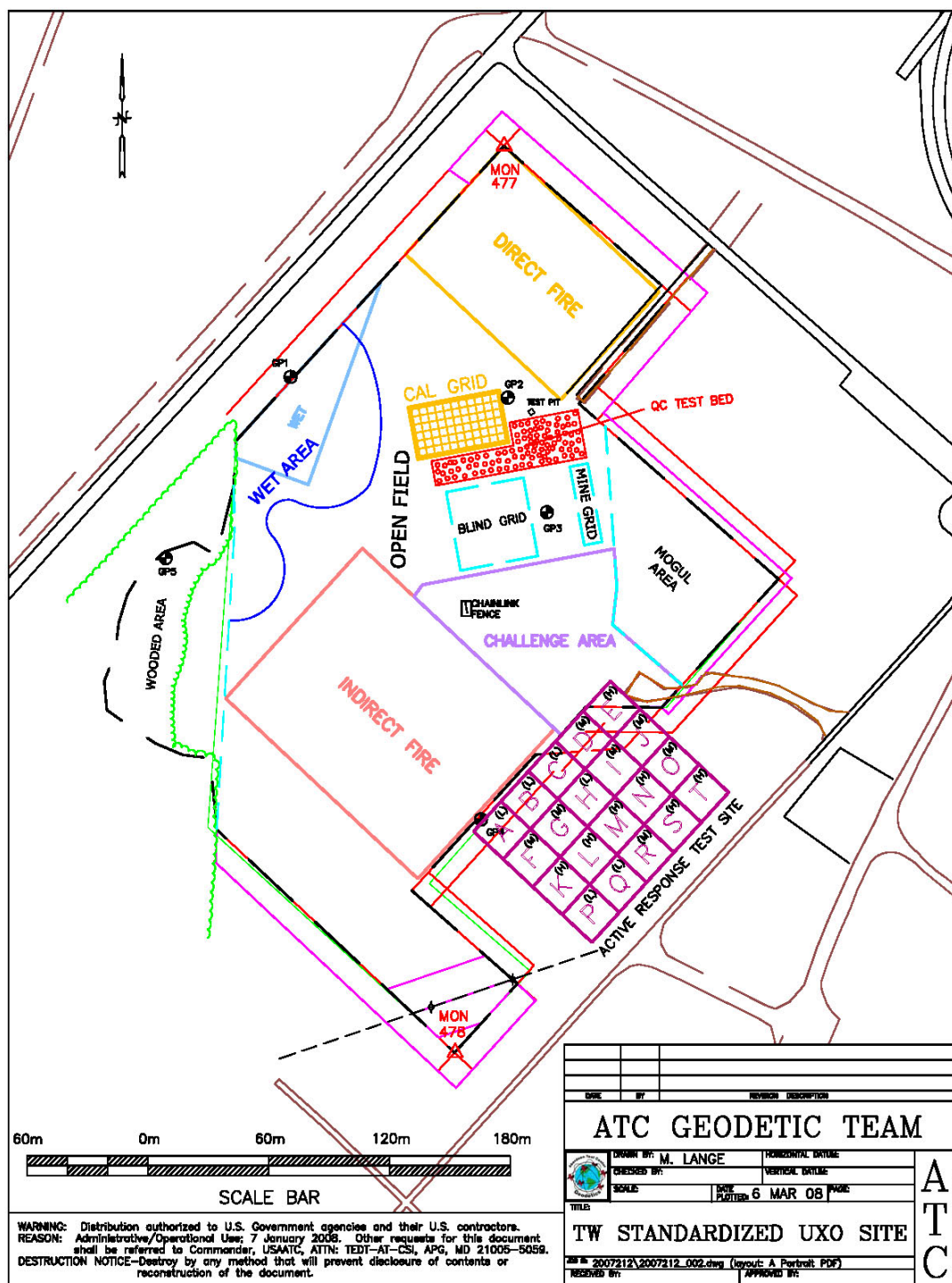


Figure 4-1 – Map of the reconfigured APG Standardized UXO Test Site.

## **4.2 FORMER CAMP SAN LUIS OBISPO**

The site description material reproduced here is taken from the recent SI report [7]. More details can be obtained in the report. The former Camp SLO is approximately 2,101 acres situated along Highway 1, approximately five miles northwest of San Luis Obispo, California. The majority of the area consists of mountains and canyons. The site for this demonstration is a mortar target on hilltop in MRS 05 (within former Rifle Range #12).

### **4.2.1 SITE SELECTION**

This site was chosen as the next in a progression of increasingly more complex sites for demonstration of the classification process. The first site in the series, former Camp Sibert, had only one target-of-interest and item “size” was an effective discriminant. At this site, there are at least four targets-of-interest: 60-mm, 81-mm, and 4.2-in mortars and 2.36-in rockets. This introduces another layer of complexity into the process.

### **4.2.2 SITE HISTORY**

Camp SLO was established in 1928 by the State of California as a National Guard Camp. Identified at that time as Camp Merriam, it originally consisted of 5,800 acres. Additional lands were added in the early 1940s until the acreage totaled 14,959. From 1943 to 1946, Camp SLO was used by the U.S. Army for infantry division training including artillery, small arms, mortar, rocket, and grenade ranges. According to the Preliminary Historical Records Review (HRR), there were a total of 27 ranges and thirteen training areas located on Camp SLO during World War II. Construction at the camp included typical dwellings, garages, latrines, target houses, repair shops, and miscellaneous range structures. Following the end of World War II, a small portion of the former camp land was returned to its former private owners. The U.S. Army was making arrangements to relinquish the rest of Camp SLO to the State of California and other government agencies when the conflict in Korea started in 1950. The camp was reactivated at that time.

The U.S. Army used the former camp during the Korean War from 1951 through 1953 where the Southwest Signal Center was established for the purpose of signal corps training. The HRR identified eighteen ranges and sixteen training areas present at Camp SLO during the Korean War. A limited number of these ranges and training areas were used previously during World War II. Following the Korean War, the camp was maintained in inactive status until it was relinquished by the Army in the 1960s and 1970s. Approximately 4,685 acres was relinquished to the General Services Administration (GSA) in 1965. GSA then transferred the property to other agencies and individuals beginning in the late-1960s through the 1980s; most of which was transferred for educational purposes (California Polytechnic State University and Cuesta College). A large portion of Camp SLO (the original 5,880 acres) has been retained by the California National Guard (CNG) and is not part of the FUDS program.

### 4.2.3 SITE TOPOGRAPHY AND GEOLOGY

The former Camp SLO site consists mainly of mountains and canyons classified as grassland, wooded grassland, woodland, or brush. A major portion of the site is identified as grassland and is used primarily for grazing. Los Padres National Forest (woodland) is located to the north-northeastern portion of the site. During the hot and dry summer and fall months, the intermittent areas of brush occurring throughout the site become a critical fire hazard.

The underlying bedrock within the former Camp SLO site area is intensely folded, fractured, and faulted. The site is underlain by a mixture of metamorphic, igneous, and sedimentary rocks less than 200 million years old. Scattered throughout the site are areas of fluvial sediments overlaying metamorphosed material known as Franciscan mélangé. These areas are intruded by plugs of volcanic material that comprise a chain of former volcanoes extending from the southwest portion of the site to the coast. Due to its proximity to the tectonic interaction of the North American and Pacific crustal plates, the area is seismically active.

A large portion of the site consists of hills and mountains with three categories of soils occurring within: alluvial plains and fans; terrace soils; and hill/mountain soils. Occurring mainly adjacent to stream channels are the soils associated with the alluvial plains and fans. The slope is nearly level to moderately sloping and the elevation ranges from 600 to 1,500 feet. The soils are very deep and poorly drained to somewhat excessively drained. Surface layers range from silty clay to loamy sand. The terrace soils are nearly level to very steep and the elevations ranges from 600 to 1,600 feet. Soils in this unit are considered shallow to very deep, well drained, and moderately well drained. The surface layer is coarse sandy loam to shaley loam. The hill/mountain soils are strongly sloping to very steep. The elevation ranges from 600 to 3,400 feet. The soils are shallow to deep and excessively drained to well drained with a surface layer of loamy sand to silty clay.

### 4.2.4 MUNITIONS CONTAMINATION

A large variety of munitions have been reported as used at the former Camp SLO. Munitions debris from the following sources was observed throughout MRS 05 during the 2007 SI:

- 4.2-inch white phosphorus mortar
- 4.2-inch mortar base plate
- 3.5-inch rocket
- 37mm projectile
- 75mm projectile
- flares found of newer metal; suspected from CNG activities
- 105mm projectile
- 60mm mortar
- 81mm mortar
- Practice bomb
- 30 cal. casings and fuzes

At the particular site of this demonstration, 60-mm, 81-mm, and 4.2-in mortars and mortar fragments have been observed. During the initial EM61 MkII cart survey, two 2.36-in rockets were found on the surface. The excavation of two 50' x 50' grids in October 2008, as part of the

preparatory activities, has confirmed these observations and provided information on the depths of munitions at this target site.

#### 4.2.5 SITE GEODETIC CONTROL INFORMATION

The 11.8-acre demonstration site is shown in Figure 4-2 as a series of included 30m x 30m cells with a topographical map as the background. The cells are color-coded based on the data collection systems that collected data on them, tan color for all systems and blue for vehicular systems only. An interior area is excluded due to rock outcroppings and the local slope. There are three control point monuments available near the site for use as GPS base station points established by Cannon Associates, of San Luis Obispo, CA referenced against nearby CALTRANS monument “A1315” [8]. The positions are listed in Table 4-2. Figure 4-3 shows the locations of monuments “A1315” and “ESTCP” with respect to the demonstration site. Monuments “MM” and “BUD” are located within 10m of “ESTCP” and are not shown for clarity. The horizontal datum for all values is NAD83. The vertical control is referenced to the NAVD88 datum and the Geoid03 geoid. Latitude and Longitude are given in degrees / minutes / seconds. Northing and Easting values are given in UTM Zone 10 (meters).

Table 4-2 – Geodetic Control at the former Camp San Luis Obispo Demonstration Site

ID	Latitude (NAD83, deg)	Longitude (deg) (NAD83, deg)	Elevation (m)	Northing (UTM Zone 10, m)	Easting (UTM Zone 10, m)	HAE (m)
ESTCP	35° 20' 37.77465" N	120° 44' 25.95073" W	113.69	3,913,515.94	705,330.89	76.01
MM	35° 20' 37.53766" N	120° 44' 25.89483" W	113.54	3,913,508.67	705,332.47	75.81
BUD	35° 20' 37.61603" N	120° 44' 26.18134" W	113.66	3,913,510.92	705,325.18	75.93

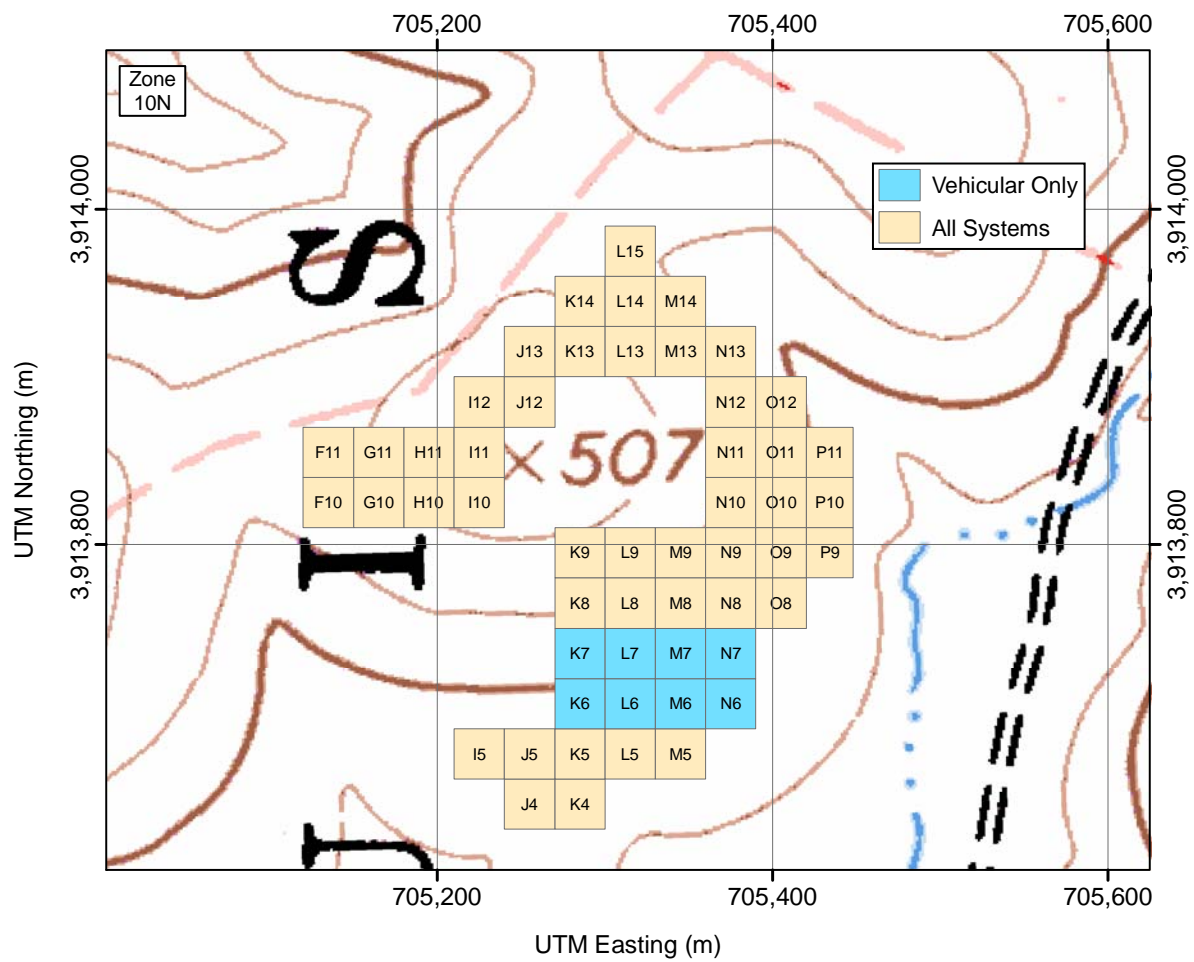


Figure 4-2 – ESTCP UXO Classification Study demonstration site at the former Camp San Luis Obispo. The site is shown as a series of included 30m x 30m cells. See the text for further discussion.

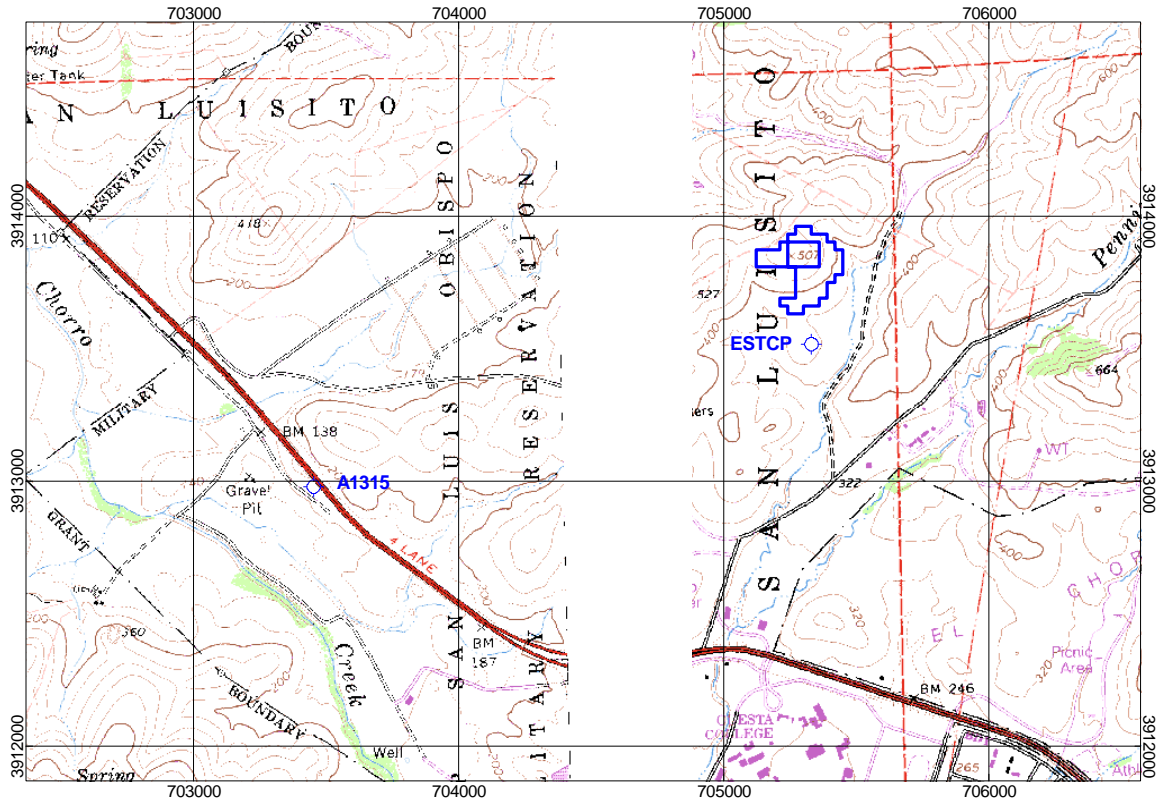


Figure 4-3 – Locations of two GPS control points with respect to former Camp SLO demonstration site

## 4.2.6 SITE CONFIGURATION

The demonstration site was configured as a single 11.8 acre area as shown in Figure 4-2. The site spans a significant fraction of the hillside that is the historical mortar target. The test pit was located near the logistics base and the calibration strip was located outside the inner fence line, convenient to the site access road.

## 5.0 TEST DESIGN

### 5.1 CONCEPTUAL EXPERIMENTAL DESIGN

Each demonstration was designed to be executed in two stages. The first stage consisted of a standard MTADS dynamic survey of site. For the APG demonstration, the MTADS magnetometer array was the survey instrument. The details of the magnetometer survey can be found in Reference 9. For the former Camp SLO demonstration, the MTADS EM61 MkII array was the survey instrument. The details of the MkII survey can be found in Reference 10.

Anomaly locations were identified from the survey data in a combination automated / manual method as described in Section 6.2. A data segment around each anomaly center was extracted and analyzed using the UX-Analyze subsystem of the Oasis montaj software package as

described in Section 6.2 to fit the data to a dipole model and extract the associated fit parameters (position, depth, equivalent size). These fit results constituted the source anomaly list for the second stage of each demonstration.

This method relies on the establishment of an anomaly detection threshold. At the former Camp Sibert demonstration site, a single munitions type was present. Pit measurements at various depths and orientations of an example article were made and bounding response curves generated for the 4.2-in mortar, the munitions of interest. The anomaly detection threshold was then set based on the least-favorably predicted response at the USACoE standard 11x depth. These demonstration sites each contained different mixes of emplaced munitions and suspected existing munitions contamination. Individual anomaly detection thresholds were established for each site/area based on sets of pit measurements made at Blossom Point for each of the emplaced items. For each site/area, the smallest appropriate least-favorable response will be used to determine the threshold. The details of the anomaly selection process, including the response curves can be found in the demonstration data reports [9,10].

The second stage of each demonstration was the survey of each site/area using the TEMTADS array developed as part of ESTCP Project MM-0601. The array was positioned roughly over the center of each anomaly on the source anomaly list and a data set collected. Each data set was then inverted using the data analysis methodology discussed in Section 5.6.2, estimated target parameters determined, and ultimately a classification made for each anomaly. The resulting prioritized dig lists were then submitted to either the ATC or IDA for scoring and performance assessment.

## **5.2 SITE PREPARATION**

Each demonstration site had been previously configured with clearly-marked calibration and open field scenarios. At least one GPS control point was provided at each site. Basic facilities such as portable toilets and field buildings were provided at APG and acquired for SLO. Secure storage for larger vehicles and sensor arrays was limited at both sites. A 40-foot shipping container was mobilized to the site for the duration of each demonstration to provide convenient, secure storage for the MTADS tow vehicle and the sensor trailer. The container was removed at the end of each demonstration.

## **5.3 SYSTEMS SPECIFICATION**

This demonstration was conducted using the NRL MTADS tow vehicle and subsystems. The tow vehicle and each subsystem are described further in the following sections.

### **5.3.1 MTADS Tow Vehicle**

The MTADS has been developed with support from ESTCP. The MTADS hardware consists of a low-magnetic-signature vehicle that is used to tow the different sensor arrays over large areas (10 - 25 acres / day) to detect buried UXO. The MTADS tow vehicle and magnetometer array are shown in Figure 5-1.



Figure 5-1 – MTADS tow vehicle and magnetometer array.

### 5.3.2 RTK GPS System

Positioning is provided using cm-level Real Time Kinematic (RTK) Global Positioning System (GPS) receivers. To achieve cm-level precision, a fixed reference base station is placed on an established first-order survey control point near the survey area. The base station transmits corrections to the GPS rover at 1 Hz via a radio link (450 MHz).

The TEMTADS array is located in three-dimensional space using a three-receiver RTK GPS system shown schematically in Figure 2-3 [11]. The three-receiver configuration extends the concept of RTK operations from that of a fixed base station and a moving rover to moving base stations and moving rovers. The lead GPS antenna (and receiver, Main) receives corrections from the fixed base station at 1 Hz. The corrected position of the Main GPS antenna is reported at 10-20 Hz using a vendor-specific NMEA-0183 message format (PTNL,GGK or GGK). The Main receiver also operates as a ‘moving base,’ transmitting corrections (by serial cable) to the next GPS receiver (AVR1) which uses the corrections to operate in RTK mode.

A vector (AVR1, heading (yaw), angle (pitch), and range) between the two antennae is reported at 10 Hz using a vendor-specific NMEA-0183 message format (PTNL,AVR or AVR). AVR1 also provides ‘moving base’ corrections to the third GPS antenna (AVR2) and a second vector (AVR2) is reported at 10 Hz. All GPS measurements are recorded at full RTK precision, ~2-5 cm. The GPS position is averaged for 2 seconds as part of the data acquisition cycle. The averaged position and orientation information are then recorded to the position data file.

### 5.3.3 Time-Domain Electromagnetic Sensor

The TEMTADS array is a 5 x 5 square array of individual sensors. Each sensor has dimensions of 40 cm x 40 cm, for an array of 2 m x 2 m overall dimensions. The rationale of this array design is discussed in Reference 12. The result is a cross-track and down-track separation of 40 cm. Sensor numbering is indicated in Figure 2-3. The transmitter electronics and the data acquisition computer are mounted in the tow vehicle. Custom software written by NRL provides

both navigation to the individual anomalies and data acquisition functionality. After the array is positioned roughly centered over the center of the anomaly, the data acquisition cycle is initiated. Each transmitter is fired in a sequence winding outward from the center position (12) in a clockwise direction. The received signal is recorded for all 25 Rx coils for each transmit cycle. The transmit pulse waveform duration is 2.7s (0.9s block time, 9 repeats within a block, 3 blocks stacked, with a 50% duty cycle). While it is possible to record the entire decay transient at 500 MHz, we have found that binning the data into 115 time gates simplifies the analysis and provides additional signal averaging without significant loss of temporal resolution in the transient decays [13]. The data are recorded in a binary format as a single file with 25 data points (one data point per Tx cycle). The filename corresponds to the anomaly under investigation.

## **5.4 CALIBRATION ACTIVITIES**

For the TEMTADS array, a significant amount of data has been collected with the system as configured at our Blossom Point facility, both on a test stand and in the towed configuration on our test field [14]. These data and the corresponding fit parameters provide us with a set of reference parameters including those of clear background (i.e. no anomaly present).

At APG, daily calibration efforts consisted of collecting background (no anomaly) data sets at the beginning and end of each survey day and periodically throughout the day at quiet spots to determine/monitor the system noise floor. A canonical reference object, a 4" Al sphere, was placed in the test pit located near the Calibration Area and measured each day to monitor the daily variation in the system response. These two types of measurements constituted the daily calibration activities.

The sphere measurements are background subtracted and inverted to obtain the target polarizabilities. These data allow us to calibrate our sensor response in two separate ways. First, by comparing the polarizabilities derived from each separate measurement, we can monitor the daily variation in the system response. In Figure 5-2, we plot the average polarizability for all sphere measurements obtained during our entire run as a function of decay time. Variations of less than 10% of the reference values were observed over the course of eight days.

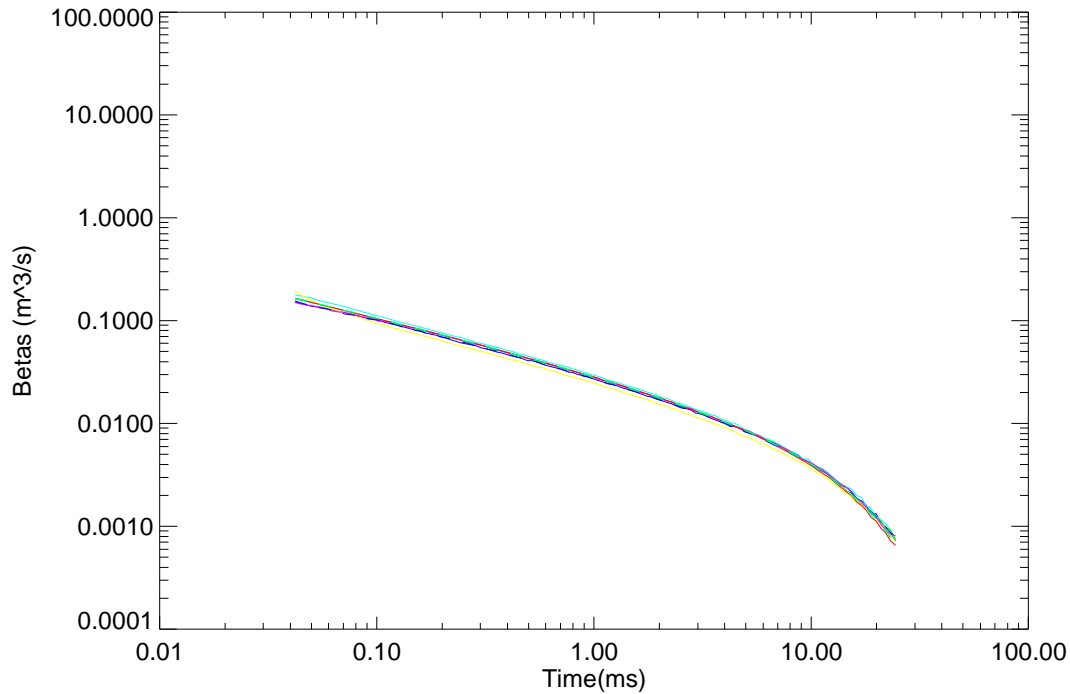


Figure 5-2 – Average polarizability for all measurements at APG of the 4” Aluminum sphere as a function of decay time

Second, we compared our derived polarizabilities directly with the predicted decay of the sphere. The theoretical decay depends on the target’s size and conductivity. We have determined this latter value for the sphere by careful measurements with a host of sensors over the years. The theoretical decay is then calculated and the derived polarizabilities are scaled in amplitude to produce the best match. Figure 5-3 shows the result for one measurement.

As this was the first demonstration of the TEMTADS array, the effect of background variation from point to point and over time was not fully understood and remains an object of study. As such, frequent backgrounds were taken over the course of each field day for immediate use for background subtraction and future analysis regarding issues of background variability and the impact on fit parameter extraction. Nine background locations were identified from the magnetometer data as being ‘quiet’ or having a very low background response level. The selected locations were positioned throughout the site to minimize the drive time to a background point from any position on the field. Additional details on system calibration at APG can be found in Reference 9.

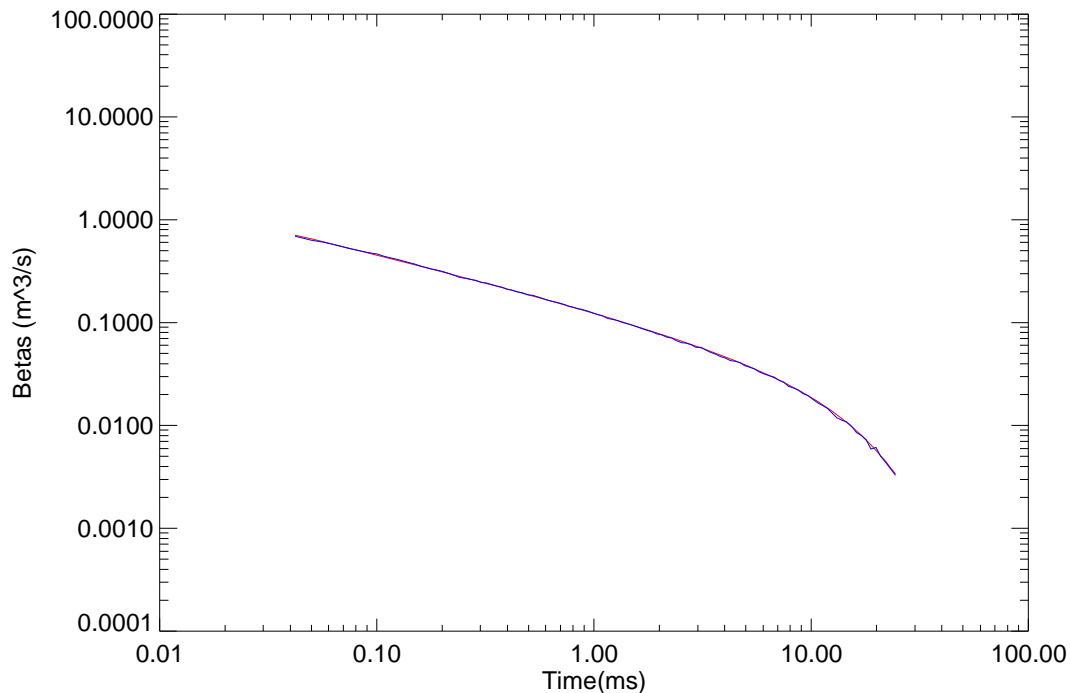


Figure 5-3 – Comparison of measured (blue) versus theoretical (red) polarizability as a function of time for the 4” Aluminum sphere

At the former Camp SLO, a calibration strip comprised of two replicates of each item of interest was emplaced on site to verify proper system operation on a daily basis. The calibration strip was surveyed each morning and each evening that data are collected. The data were preprocessed, checked for data quality, and then the signal strengths and noise levels compared to the site-specific response curves and background levels to verify consistency of system performance. Please refer to the ESTCP UXO Classification Study Demonstration Plan and the MTADS Magnetometer / EM61 MKII Demonstration Data Report [10] for further details.

## 5.5 DATA COLLECTION

### 5.5.1 Scale of Demonstration

The APG demonstration was conducted at the APG Standardized UXO Test Site. A magnetometer survey was conducted on the Calibration and Blind Grids, as well as the Indirect Fire Area (approximately 4.3 acres) on May 7, 2008. The TEMTADS array surveyed the Calibration and Blind Grids. The array was also deployed to approximately 700 anomalies in the Indirect Fire Area that were detected from the magnetometer data set. The TEMTADS array portion of the demonstration occurred from June 16 – 23, 2008.

A cued discrimination survey of the former Camp SLO demonstration was conducted within the 11.8 acre final demonstration site of approximately 1,500 previously-identified anomalies from the anomaly list generated from the MTADS EM61 MkII data set. This survey was conducted

using the NRL TEMTADS. Characterization of the system responses to the items of interest was determined using on site measurements (both pit data and calibration strip). The data segment (chip) for each anomaly was analyzed, and dipole model fit parameters extracted.

### **5.5.2 Sample Density**

Magnetometer data were collected with nominal down-track spacing of 6 cm and cross track spacing of 25 cm. EM61 MkII EMI data were collected with a nominal down-track spacing of 15 cm and a cross track spacing of 50 cm. Two orthogonal surveys were conducted to increase target illumination and data density. The EMI data spacing for the TEMATDS is fixed at 40 cm in both directions by the array design.

### **5.5.3 Quality Checks**

Preventative maintenance inspections were conducted continually by all team members during data collection, focusing particularly on the tow vehicle and sensor trailer. Deficiencies were addressed according to the severity of the deficiency. Parts, tools, and materials for many maintenance scenarios are available in the system spares inventory, a fraction of which was on site at APG due to the proximity of our base of operations at Blossom Point, MD. Please refer to the Demonstration Data Reports for further details on the survey instrument QC procedures.

Since the TEMTADS operates in a cued mode, the data QC procedures and checks differ from that of the survey mode instruments. The status of the RTK GPS system can be visually determined by the operator prior to starting the data collection cycle, assuring that the position and orientation information are valid (FQ 3) during the collection period.

Two data quality checks were performed on the TEMTADS data. After background subtraction, contour plots of the signal were generated for the 25 transmit/receive pairs at a decay time of 0.042 ms. An example of a good data set from a single anomaly with a large SNR is shown in Figure 5-4 for Calibration Area item I6. The plots were visually inspected to verify that there was a well defined anomaly without extraneous signals or dropouts. QC on the transmit/receive cross terms was based on the dipole inversion results. Our experience has shown that data glitches show up as reduced dipole fit coherence. No data glitches were observed during our APG demonstration, so data collected at our Blossom Point facility for a 105mm HEAT Projectile are used as an example. The fit polarizabilities as a function of decay time are shown with all elements (Figure 5-5) and with element 21 excluded (Figure 5-6), with fit coherences of 0.699 and 0.992 respectively. In comparing Figure 5-5 and Figure 5-6, the expected axial symmetry of the minor polarizabilities is restored with the exclusion of element 21 in this case. The problem with element 21 is only observable at late time and therefore would not be captured in the monostatic plot review.

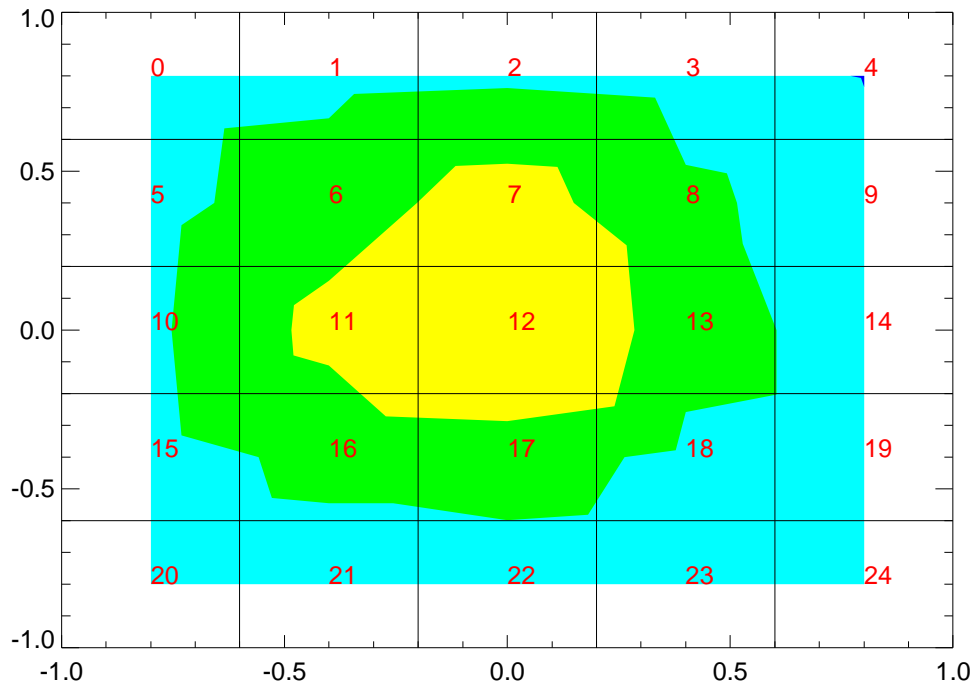


Figure 5-4 – Monostatic QC contour plot for Calibration Area item I6

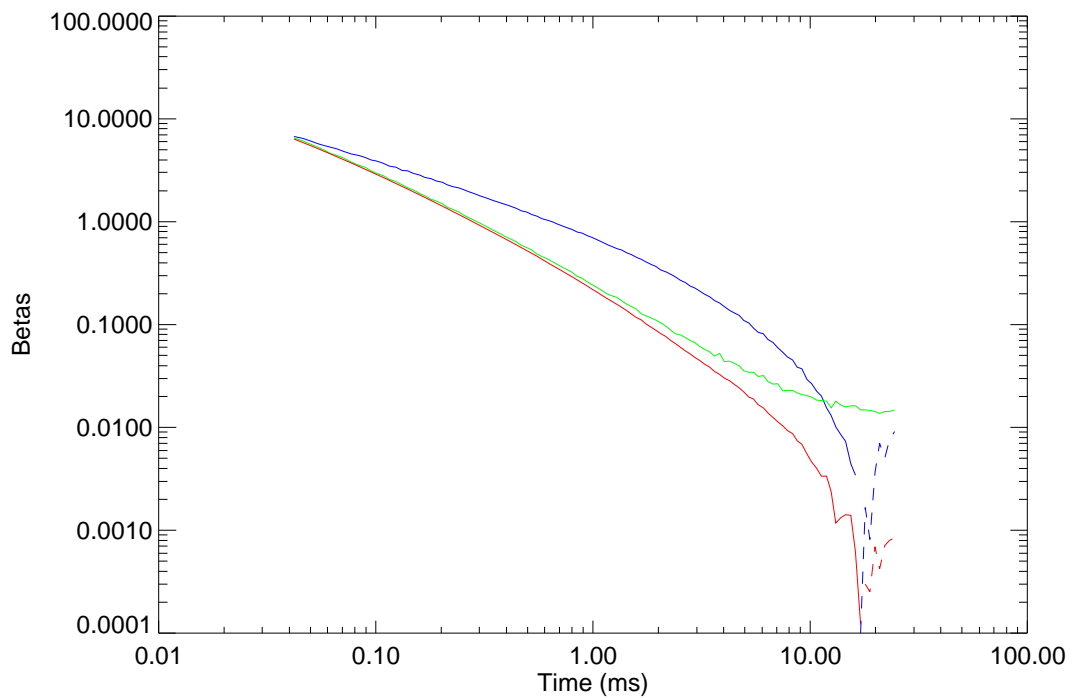


Figure 5-5 – Polarizability as a function of time for a 105mm HEAT Projectile with all data included. The fit coherence for all elements included was 0.699.

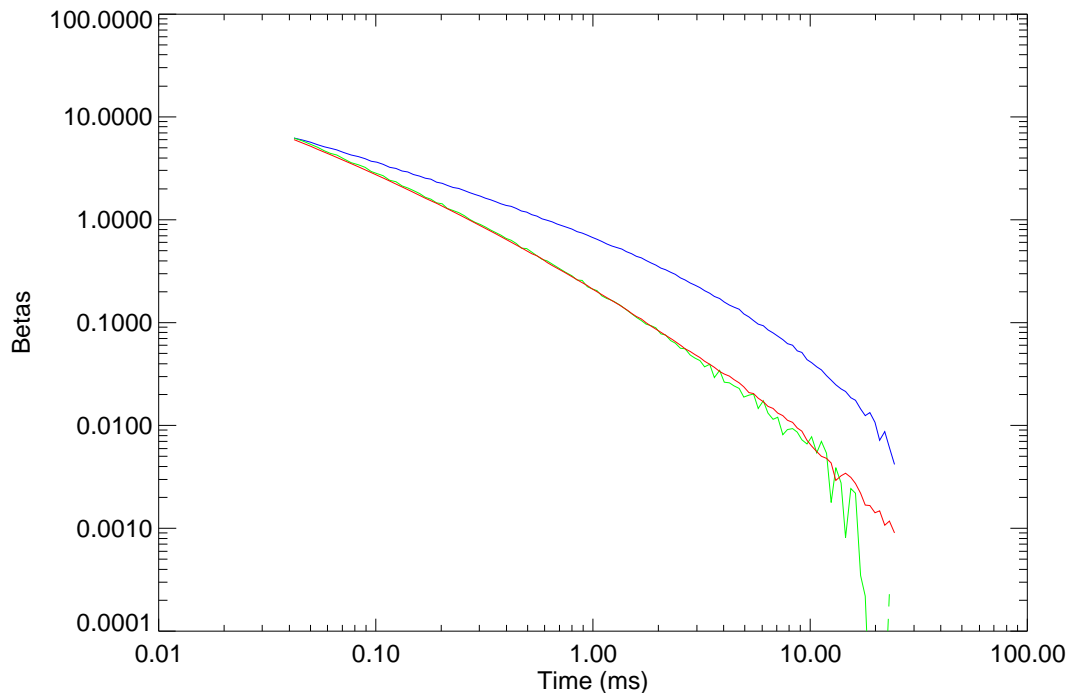


Figure 5-6 – Polarizability as a function of time for a 105mm HEAT Projectile with element 21 excluded. The fit coherence with element 21 excluded was 0.992.

The issue of when multiple objects are found to be under the array simultaneously, generating overlapping signatures, can also be addressed at this point in the data QC process. An example case is shown in Figure 5-7. There are two apparent issues in the data set. First, there appears to be a small, shallow bit of scrap on top of the target. Second, there was a bit of scrap present in the background file used. This latter issue is seen in the data from element 0. Figure 5-8 shows the fit betas obtained using all of the data. Figure 5-9 shows the fit betas obtained excluding elements 0,5,10,11,15,16,17,20,21,22. The latter betas match our library 105mm HEAT betas very well.

Any data set that was deemed unsatisfactory by the data analyst was flagged and not processed further. The anomaly corresponding to the flagged data was logged for future re-acquisition. Data which meet these standards are of the quality typical of the MTADS system.

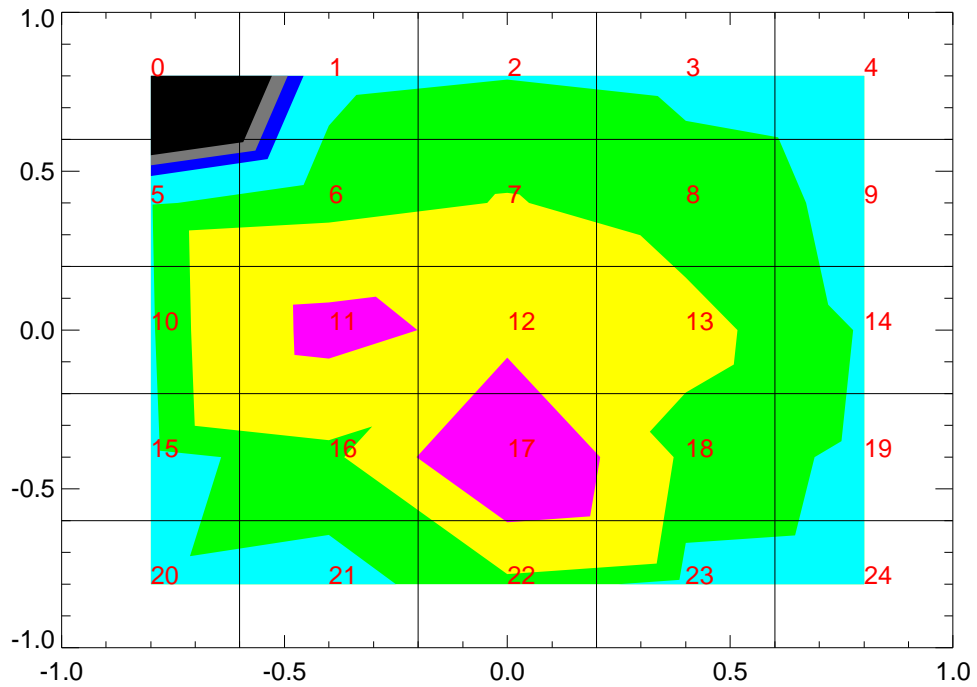


Figure 5-7 – Monostatic QC contour plot for example anomaly

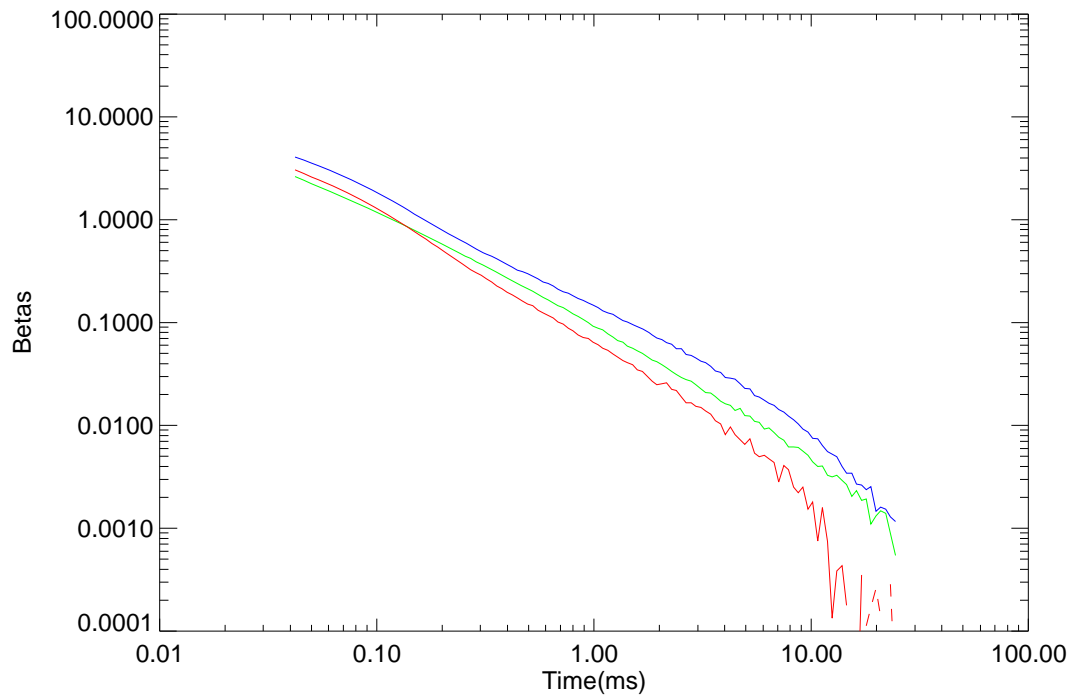


Figure 5-8 – Polarizability as a function of time for the example show in Figure 5-7 with all data included. The fit coherence for all elements included was 0.652.

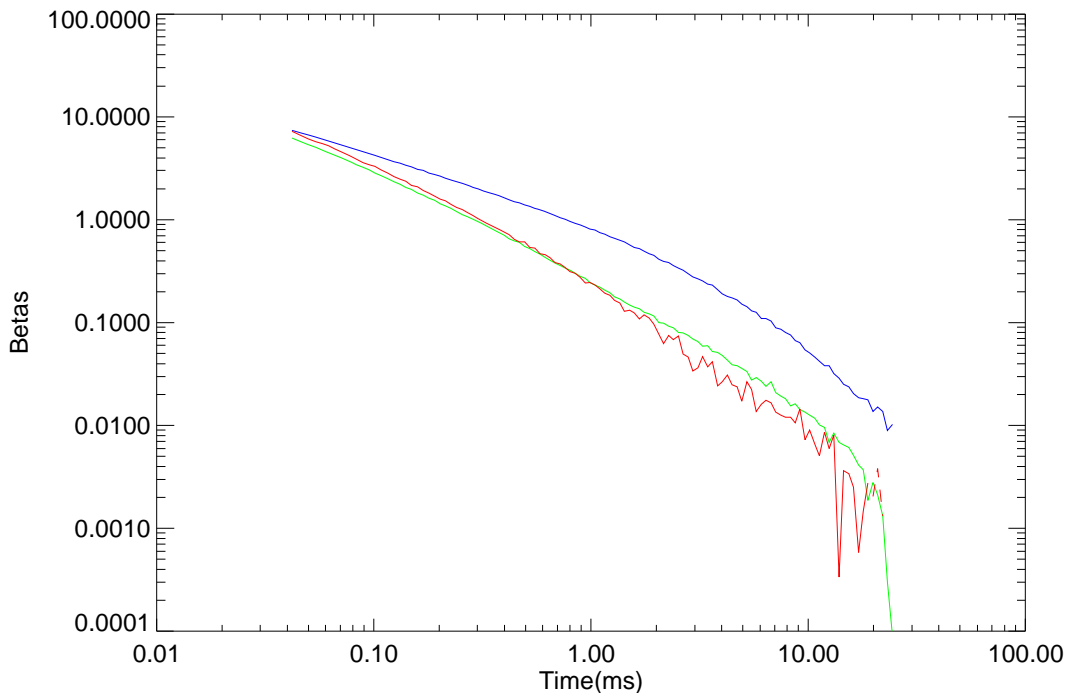


Figure 5-9 – Polarizability as a function of time for the example show in Figure 5-7 with elements 0,5,10,11,15,16,17,20,21,22 excluded. The fit coherence for the remaining elements was 0.985.

#### 5.5.4 Data Handling

Data were stored electronically as collected on the MTADS vehicle data acquisition computer hard drives. Approximately every two survey hours, the collected data were copied onto removable media and transferred to the data analyst for QC/analysis. The data were moved onto the data analyst's computer and the media recycled. Raw data and analysis results were backed up from the data analyst's computer to optical media (CD-R or DVD-R) or external hard disks daily. These results are archived on internal file servers at NRL or SAIC. All field notes / activity logs were written in ink and stored in archival laboratory notebooks. These notebooks are archived at NRL or SAIC. Relevant sections are reproduced in demonstration reports such as this. Dr. Tom Bell is the POC for obtaining data and other information. His contact information is provided in Appendix A of this report.

#### 5.5.5 APG Discrimination Survey Data Summary

The MTADS tow vehicle and TEMTADS array were mobilized to the APG Test Site during the week of June 9, 2008. The TEMTADS array portion of the demonstration commenced on June 16, 2008 with a data collection in the Calibration Area. Cued surveys were conducted of the Calibration, Blind Grid, and the Indirect Fire Area. Data collection was completed on June 23, 2008. The system was demobilized later that week to our Blossom Point facilities.

The array was positioned roughly over the center of each anomaly on the source anomaly list for each area and a data set collected. Each data set was then inverted using the data analysis methodology discussed in Section 5.6.2, estimated target parameters determined, and ultimately a classification made for each item for the Blind Grid and Indirect Fire Area.

#### **5.5.5.1. Calibration Area**

The ground truth for the Calibration Area is known and the collected data were used to verify the operational status of our systems and processing procedures. Each of the 66 seed locations in the Calibration Area was investigated in turn and the resultant fit parameters used to cross-check against and augment our library of responses to known munitions items. Data collection occurred on June 16, 2008.

#### **5.5.5.2. Blind Grid**

The Blind Grid is composed of 400 cells in a 20x20 array with 2m on-center spacing. The Rank 1 and 2 anomalies (214 anomalies) identified in the magnetometer survey (See Reference 9) formed the Blind Grid anomaly list for the TEMTADS array. ATC staff placed a plastic pin flag on the center of each of the 214 anomalies investigated prior to this portion of the demonstration. Data collection occurred during the period June 16 - 17, 2008. The background-corrected data set for each anomaly is included on the accompanying DVD.

#### **5.5.5.3. Indirect Fire Area**

The Indirect Fire Area is a 1.3 ha area drawn from the original configuration's Open Field. The IDF has been seeded with three munitions types, the 60mm and 81mm Mortar and the 105mm Projectile. The 694 anomalies in Ranks 1, 2, 3, and 7 (See Reference 9) were added to the IDF anomaly list for the TEMTADS array. Data collection occurred during the period June 17 - 23, 2008.

### **5.5.6 Former Camp San Luis Obispo**

The MTADS tow vehicle and the TEMTADS array were mobilized to the former Camp SLO along with the other MTADS systems in May, 2009. The TEMTADS portion of the demonstration commenced on June 8, 2009. Cued surveys were conducted for approximately 1,500 anomalies identified from the MTADS EM61 MkII array survey data. The Calibration Strip was surveyed twice daily, once at the beginning and once at the end of the survey day. Data collection was completed on June 18, 2009. The system was demobilized later that week to our Blossom Point facilities.

The array was positioned roughly over the center of each anomaly on the source anomaly list and a data set collected. Each data set was then inverted using the data analysis methodology discussed in Sections 6.1 and 6.3, estimated target parameters determined, and ultimately a classification made for each entry on the anomaly list.

#### **5.5.6.1. Calibration Strip**

A calibration strip, comprised of two samples of each of the four targets of interest plus two shotputs, was emplaced on site as a means of verifying proper system operation on a daily basis. The strip was surveyed twice daily, once at the beginning of the day, and once at the end. The sole exception to this procedure occurred on our third day, when brake problems with the vehicle forced an early cessation of activities. The measured peak signal for each emplaced item was determined for each run and compared over the course of the demonstration to insure the reproducible, physically realistic performance of the sensor array. The results are discussed in Section 7.0.

#### **5.5.6.2. Main Demonstration**

The former Camp SLO demonstration site was 11.8 acre area as shown in Figure 4-2. A total of 1547 anomalies (including reacquisitions requested by the Data Analyst) were measured over a period of 10 days for an average of 155 anomalies/day. The only days for which our average fell below our goal of 125 anomalies/day were the final day, due to completing the data collection, and 2 other days in which necessary vehicle maintenance shortened our workday.

### **5.6 VALIDATION**

#### **5.6.1 Aberdeen Proving Grounds**

With the exception of the Calibration Grid, the ground truth for the Standardized sites is held back from individual technology demonstrators to preserve the utility of the Blind Grid and Open Field Areas. Results from the Blind Grid and the Indirect Fire Area were submitted to ATC for performance evaluation. Scoring results have been received and are available [15]. A summary of the results are given in Section 7.0.

#### **5.6.2 Former Camp San Luis Obispo**

At the conclusion of data collection activities, all anomalies on the master anomaly list assembled by the Program Office were excavated. Each item encountered was identified, photographed, its depth measured, its location determined using cm-level GPS, and the item removed if possible. All non-hazardous items were saved for later in-air measurements as appropriate. This ground truth information, once released, was used to validate the objectives listed in Section 3.2.

## **6.0 DATA ANALYSIS AND PRODUCTS**

The TEMTADS is a cued UXO classification system. There were two parts to the data collection in each demonstration: an initial survey which served primarily to locate targets, and TEMTADS measurements made over the each target detected in the survey. The TEMTADS data were used for target classification and discrimination.

## 6.1 PREPROCESSING

The collected survey data were preprocessed on site for quality assurance purposes using standard TEMTADS procedures and checks as discussed in Section 5.5.3 and References 9 and 19.

The TEMTADS has 25 transmitters/receiver pairs. For each transmit pulse, the response measured at all of the receivers was recorded simultaneously. For each target, a  $25 \times 25 \times N$  data array is generated, where  $N$  is the number of recorded time gates. The current system configuration bins the data in 121 logarithmically spaced gates. During the preprocessing step, the recorded signals are normalized by the transmitter currents to account for any transmitter variations. To account for time delay due to effects of the receive coil and electronics, we subtract 0.028 ms from the nominal gate times [16]. The delay was previously determined empirically by comparing measured responses for test spheres with theory. The measured responses include distortions due to transmitter ringing and related artifacts out to about 40  $\mu$ s. Consequently we only included the responses from decay times beyond 40  $\mu$ s in our analyses. This leaves 115 gates spaced logarithmically between 0.042 ms and 25 ms.

The background response was subtracted from each target measurement using data collected in a nearby target-free region, or background. Background locations were selected from quiet areas observed in the magnetometer anomaly map. All of the background measurements were inter-compared to evaluate background variability and to identify outlier measurements potentially corresponded to measurements over non-ferrous targets. We have not observed significant background variability in our measurements at our Blossom Point test site, and were able to use blank ground measurements from 100 meters away for background subtraction on targets in the test field.

Geo-referencing of the array data is based on the GPS data, which gives the location of the center of the array and the orientation of the array. Sensor locations within the array are fixed by the array geometry. Dipole inversion of the array data (Section 6.3) determines target location in local array-based coordinates. The local position was then transformed to absolute coordinates using the array location and orientation determined from the corresponding GPS data.

## 6.2 TARGET SELECTION FOR DETECTION

Targets were selected from the survey data using the threshold exceedance methods described in References 9 and 10 using a physics-based threshold in Oasis montaj. The data chips associated with the detected anomalies were then processed in an automatic processing mode of UX-Analyze. The results of the automatic processing were then reviewed in UX-Analyze's interactive mode to allow operator experience to be included in the target selection. In the case of the APG demonstration, a small number of additional anomalies were identified by the operator and added to the anomaly list. For the former Camp SLO demonstration, the operator coalesced double-peaked features into a single anomaly where appropriate.

The UX-Analyze environment for anomaly review contains two main graphics tools. One displays an interpolated amplitude image of all the data processed at the site for the current survey and allows the analyst to see which grids of the site have been surveyed and to select grids for target analysis. The area selected for analysis is displayed in another graphic window in which the analyst visually selects targets for review. In both of these windows there are options for changing the view area, the mapping color palette and contrast, the amount of information overlaid on the screen, etc. To refine a characterization of a target, the analyst modifies the data boundary using the mouse. When the boundary is closed, the data inside are sent to a dipole fitting algorithm to determine target parameters such as location, depth and apparent size. The anomaly lists were then sorted prioritized dig lists.

### 6.3 PARAMETER ESTIMATION

The raw signature data from the TEMTADS reflect details of the sensor/target geometry as well as inherent EMI response characteristics of the targets themselves. In order to separate out the intrinsic target response properties from sensor/target geometry effects we invert the signature data to estimate principal axis magnetic polarizabilities for the targets. The TEM data are inverted using the standard induced dipole response model wherein the effect of eddy currents set up in the target by the primary field is represented by a set of three orthogonal magnetic dipoles at the target location [17]. The measured signal is a linear function of the induced dipole moment  $\mathbf{m}$ , which can be expressed in terms of a time dependent polarizability tensor  $\mathbf{B}$  as

$$\mathbf{m} = \mathbf{U}\mathbf{B}\mathbf{U}^T \cdot \mathbf{H}_0$$

where  $\mathbf{U}$  is the transformation matrix between the physical coordinate directions and the principal axes of the target and  $\mathbf{H}_0$  is the primary field strength at the target. The eigenvalues  $\beta_i(t)$  of the polarizability tensor are the principal axis polarizabilities.

Given a set of measurements of the target response with varying geometries or "look angles" at the target, the data can be inverted to determine the (X,Y,Z) location of the target, the orientation of its principal axes ( $\phi, \theta, \psi$ ), and the principal axis polarizabilities ( $\beta_1, \beta_2, \beta_3$ ). The basic idea is to search out the set of nine parameters (X,Y,Z, $\phi, \theta, \psi, \beta_1, \beta_2, \beta_3$ ) that minimizes the difference between the measured responses and those calculated using the dipole response model.

For the TEMTADS data, inversion is accomplished by a two-stage method. In the first stage, the target's (X,Y,Z) dipole location is solved for non-linearly. At each iteration within this inversion, the nine element polarizability tensor ( $\mathbf{B}$ ) is solved linearly. We require that this tensor be symmetric; therefore, only six elements are unique. Initial guesses for X and Y are determined by a signal-weighted mean. The routine normally loops over a number of initial guesses in Z, keeping the result giving the best fit as measured by the chi-squared value. The non-linear inversion is done simultaneously over all time gates, such that the dipole (X,Y,Z) location applies to all decay times. At each time gate, the eigenvalues and angles are extracted from the polarizability tensor.

In the second stage, six parameters are used: the three spatial parameters (X,Y,Z) and three angles representing the yaw, pitch, and roll of the target (Euler angles  $\phi, \theta, \psi$ ). Here the eigenvalues of the polarizability tensor are solved for linearly within the 6-parameter non-linear inversion. In this second stage both the target location and its orientation are required to remain constant over all time gates. The value of the best fit X, Y, and Z from the first stage, and the median value of the first-stage angles are used as an initial guess for this stage. Additional loops over depth and angles are included to better ensure finding the global minimum.

Figure 6-1 shows an example of the principal axis polarizabilities determined from TEMTADS data. The target, a mortar fragment, is a slightly bent plate about ½ cm thick, 25 cm long and 15 cm wide. The red curve is the polarizability when the primary field is normal to the surface of the plate, while the green and blue curves correspond to cases where the primary field is aligned along each of the edges.

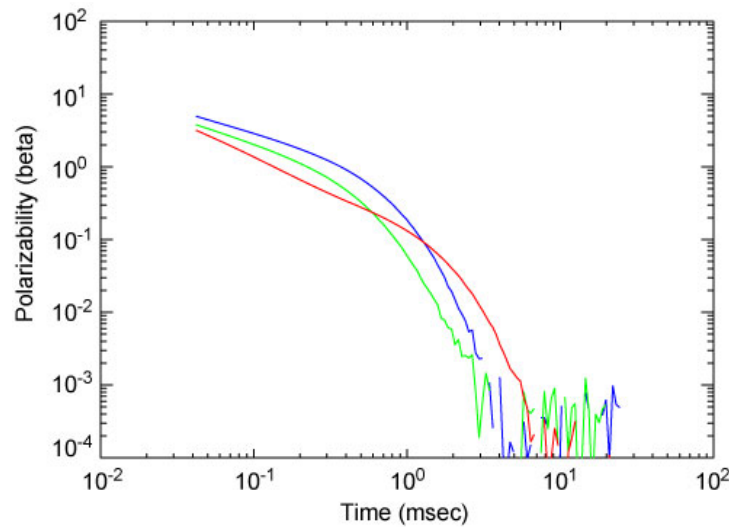


Figure 6-1 – Principal axis polarizabilities for a ½ cm thick by 25cm long by 15cm wide mortar fragment.

Not every target from the detection surveys had a strong enough TEM response to support extraction of target polarizabilities. All of the data were run through the inversion routines, and the results were manually screened to identify those targets that could not be reliably classified. Several criteria were used in this process: signal strength relative to background, dipole fit error (difference between data and model fit to data), the visual appearance of the polarizability curves.

For moderate-to-good SNR, our derived polarizabilities can be directly compared with those of our target library. In these cases, a metric was computed based on how well the amplitude and ratio of the target polarizabilities match those of library objects. The metric runs from 0 (no match) to 1 (perfect match). For the APG demonstration and targets with lower SNR, or for cases where a visual inspection suggested a match, but the match quality was below our cutoff,

target classification and discrimination were done using library matching procedures similar to those used by Sky Research, Lawrence Berkeley Lab and ourselves in the ESTCP Discrimination Study Pilot Program at the former Camp Sibert [18]. The fit quality of an unconstrained dipole inversion of the TEMTADS data was compared to the fit quality of a dipole fit constrained by a set of principal axis polarizabilities drawn from a signature library. Fit quality is the squared correlation coefficient between the model fit and the data. If the ratio of the constrained fit quality to the unconstrained fit quality ( $\rho$ ) is one, then the library item is as good a match to the data as possible. If the ratio is small, then the library item is a poor match.

The scoring rules for the SLO demonstration were different than those used for APG submissions, including the introduction of the “Can’t Decide” category discussed in the next section. Therefore a similar, but modified process was used. The primary library match algorithm compares the polarizabilities of an unknown target with each library entry based on 3 criteria: the amplitude of  $\beta_1$ , and the two shape parameters,  $\beta_2/\beta_1$  and  $\beta_3/\beta_1$ . The difference in the values is computed at all timegates, excluding those where the values are negative. The differences are then plugged into a Gaussian. The “time constants” in these Gaussians were derived by examining the variability in the amplitude and shape parameters for a large number of objects for which ground truth was known. Medians are taken to avoid bad data points. Finally, the results from the 3 different criteria are averaged, producing a metric which ranges from 0 (worst possible fit) to 1 (perfect fit). Note that the procedure just described is not a library constrained match, i.e., we do not invert our data forcing the  $\beta$ ’s to be those of each library object in turn, but rather simply compare our unconstrained polarizabilities to those of the library. As such, the comparison runs rapidly, and there is no need to reduce the number of separate types in the library to balance computation time.

For each anomaly, this match is performed on both the polarizabilities from the single dipole fit, and those of each target obtained by the multi-dipole fit. The metric is set to whichever set of  $\beta$ ’s produces the best match.

Due to the occasional “splitting” of the two smaller  $\beta$ ’s, we also considered a second metric in which the 3<sup>rd</sup> comparison, namely the  $\beta_3/\beta_1$  shape match, was dropped from the calculation. Two separate prioritized dig lists were submitted, one using the 3 criteria match metric, and one using this 2 criteria match metric.

## **6.4 CLASSIFIER AND TRAINING**

Prior to the demonstrations we collected training data in air for all of the 14 standard APG ordnance targets and the four known munitions types for the former Camp SLO site. These data were used to generate the fit library entries. Many of the targets are composites of two or more distinct parts, like a steel body combined with an aluminum tail assembly. Depending on the distance between the sensors and the target, such items can exhibit a range of slightly different EMI signatures corresponding to excitation from different directions. We included measurements with the target oriented nose up, towards the sensor array, nose down, away from the array, flat and obliquely in the fit library.

Our experience at our Blossom Point test site has been that polarizabilities determined from in-air measurements are indistinguishable from those determined from measurements taken over buried targets. We used the data collected from the site calibration areas, which contains several instances of each target, to establish that this held true.

We have assembled a fairly extensive polarizability database for clutter items recovered from several different sites. This library was used as training data for establishing UXO/clutter discrimination boundaries on the direct match metric and on the coherence ratio  $\rho$ .

As noted in Section 6.3, for anomalies with moderate-to-good SNR and no serious overlap issues, classification was done using the direct match metric, wherein the unconstrained polarizabilities are compared with those of library objects. For the APG demonstration, using the results of the Calibration Grid, and even considering Blind Grid and IDF anomalies where the visual match to a library object is so good that we have high confidence in the identification, we determined a cutoff value for our metric of 0.56 (reduced to 0.44 for the 25 mm), above which the target is considered ordnance, and below which it is considered clutter. This can be considered a first pass for classification, and was applied to all anomalies.

For the former Camp SLO demonstration, a different classification scheme was used. A series of decision rules were used to classifying anomalies into 4 categories for placement on the final, prioritized dig list. These decision rules are outlined below, as well as the criteria for determining overlapping signatures.

#### **6.4.1 Cannot Analyze**

We classified targets as “Cannot Analyze” for those which the inversion produced unphysical parameters, specifically, depths below a cutoff based on the largest target expected on the site, and negative polarizabilities. A depth value of 2m was used.

#### **6.4.2 Likely Munition**

We classified targets as “Likely Munitions” based on the library match metrics previously described. The cutoff is determined to insure that all training targets revealed as UXO or TOI with moderate-to-good signal-to-noise were included. Our cutoff values were 0.8336 for the 3 criteria metric, and 0.8925 for the 2 criteria metric.

#### **6.4.3 Cannot Decide**

Targets in this category were comprised of four distinct types. The first type consisted of targets with very low signal-to-noise, based on previous experience with this instrument. A cutoff signal amplitude value of 2mv/A was used. The second type was targets which suffered from serious overlap issues with neighboring anomalies, to the extent that we were not confident in our ability to extract meaningful features. The remaining two categories excluded cases from the first two. The third category consisted of targets whose match metric fell within a “buffer zone” below the “Likely Munition” metric cutoff. The anomalies in this category possessed a match metric which

was not sufficiently high to justify their being classified as “Likely Munitions”, but which is not sufficiently low to classify them as “Likely Clutter”. The actual values for this lower metric cutoff were determined from a visual inspection of matches in the Test Set data, and were equal to 0.7365 for the 3 criteria metric, and 0.8335 for the 2 criteria metric. Finally, the fourth type consisted of anomalies for which the metric fell below the “Likely Munition” cutoff, but which possess axial symmetry. This choice was made to take account of the fact that our library is finite. Exceptions to the axial symmetry rule were targets that showed rapid decay (based on the most rapid decay for UXO in the complete library), and targets whose polarizabilities were of very small amplitude (based on the smallest amplitude UXO in the complete library). We conservatively defined axial symmetry as a median agreement of 50% between the two smaller betas.

#### **6.4.4 Likely Clutter**

Targets were placed in this category whose metric fell below that of the second “buffer zone” cutoff and which did not show axial symmetry as previously defined.

#### **6.4.5 Ranking**

The “Likely Clutter” category was divided into two subcategories: low signal-to-noise and moderate to high signal-to-noise. Within each of these subcategories, ranking was done by the library match metric, such that the lower the metric, the higher the rank. However, all anomalies in the low SNR subcategory were ranked lower than those in the moderate to high SNR subcategory. The rationale behind this is that low SNR can decrease the quality of the match metric, and the targets for which we had the highest confidence of being clutter are those with a low metric and decent SNR. Similarly, the “Cannot Decide” category was divided into three subcategories based on the four types of entries, with the targets having low signal and overlap issues having the highest rank, followed by those with moderate-to-high signal and no serious overlap issues, with those targets having a metric above the “buffer zone” cutoff giving a lower ranking (less likely to be clutter) than those below. The ranking within each subcategory was ordered by the metric. Finally, the “Likely Munition” category was ranked solely by the metric, with the largest rank going to the largest metric value.

Since it is not obvious how to incorporate either the axial symmetry parameter, the low SNR parameter, or the overlap into our probabilities, we simply set the probability equal to the 1 minus the metric value for all targets. Unfortunately, with the exception of the “Likely Munition” category, this means that there was in general not a 1 to 1 mapping between the ranks and the probabilities.

#### **6.4.6 Determination of Overlapping Signals**

As discussed in Section 5.5.3, monostatic contour plots were made of each anomaly both as a QC check and as a means of determining whether the anomaly suffers from overlapping signatures. Thus, an entry was made in a spreadsheet giving some indication of the extent of the overlap, if any. In some cases, this overlap may have been from multiple targets within the

anomaly, as opposed to being caused by a separate anomaly. Therefore, we used this entry in conjunction with the knowledge of the location of other anomalies relative to the target of interest. The edge of the TEMTADS is 1m from a target located under the array center. Thus, we declaring any anomaly for which the spreadsheet entry indicates overlap, and for which at least one target was within 1.5m of the anomaly, as an overlapping signal.

## 6.5 DATA PRODUCTS

The data product requirements for the two demonstrations were different and different data products were correspondingly generated. For the APG demonstration, we used the standard reporting templates for the Blind Grid and the Open Field. The metrics in Section 3.0 were calculated directly from the Scoring Report provided by the Standardized Test Site administrators. The Response Stage value was the maximum signal level above background from the magnetometer anomaly. The calculation of the discrimination stage was more involved. For those targets classified as ordnance, the direct match metric was used as the ranking. Additionally, targets which we could not analyze as described in Section 6.3 were classified as ordnance, but given the lowest confidence rating, and noted as such in our submission. For targets classified as clutter, a division was made between targets that had moderate-to-good SNR and little to no overlap with adjacent targets, and those with either low SNR or more serious overlap issues. For the former class, ranking was based on the direct match metric, while for the latter, ranking was based on a combination of the direct match metric and the peak signal. Classification and Type were determined from the direct match metric or the coherence ratio  $\rho$ , as applicable. Easting, Northing, Depth, Azimuth and Dip all came from the dipole inversion results.

For the former Camp SLO demonstration, the data products were summarized in the prioritized dig list, a small section of which is reproduced in Table 6-1 as an example. The ‘decision statistic’ refers to the direct match metric described in previous sections. The ‘Rank’ column lists the anomalies from 1 to N where 1 indicates most likely non-TOI and N indicates high confidence TOI. The ‘Category’ column lists an integer key of 1 for likely clutter, 2 for Can’t Decide, 3 for likely munitions, or 4 for Can’t Analyze. The ‘Overlap’ column lists nearby anomalies (if any) that spatially overlap. The ‘Type’ column was used to list the munitions type. The Easting, Northing, Depth, Azimuth, and Dip columns reported inversion results. The ‘Items/Anomaly’ column reported an estimate of the number of sources that contributed to the observed anomaly.

Table 6-1 – Partial prioritized dig list for the former Camp SLO TEMTADS demonstration.

MASTER ID	DECISION STATISTIC	Rank	Category	Overlaps	Type	Easting (m)	Northing (m)	Depth (m)	Azimuth	Dip	Items / Anomaly
441	0.1107	1047	2	0		705280.41	3913908.62	0.559	104.94	32.94	1
538	0.1088	1048	2	0		705301.47	3913778.32	-0.083	169.97	30.3	1
783	0.1075	1049	3	41	60mm	705343.03	3913787.55	0.503	63.8	39.68	3
825	0.1072	1050	3	0	4.2in	705349.68	3913791.99	0.652	186.01	9.29	3

## **7.0 PERFORMANCE ASSESSMENT**

The TEMTADS array was constructed in 2007, field tested at the APG Standardized UXO Test Site in June 2008 [15], and participated in the ESTCP UXO Classification Study at the former Camp SLO site in June 2009 [19].

Due to the nature of the demonstrations at each site and the employed scoring methods, separate Performance Objectives are provided for each demonstration in the following subsections.

### **7.1 APG STANDARDIZED UXO TEST SITE**

For the APG demonstration, a magnetometer data set collected the previous month at the newly reconfigured test site was used for anomaly detection. Approximately 200 cells in the Blind Grid and 700 anomalies in the Indirect Fire Area were interrogated with the TEMTADS, averaging 200 anomalies/day on the Indirect Fire Area. After processing, ranked dig lists were generated and submitted to ATC for scoring.

The performance objectives for this demonstration were summarized in Table 3-1, and are repeated here as Table 7-1. The results for each criterion are then discussed in the following sections. The ATC scoring report for the demonstration, Reference 15, provides the source material for evaluating several of the performance objectives.

Table 7-1 – Performance Results for the APG Demonstration

Performance Objective	Metric	Data Required	Success Criteria	Success?
<b>Quantitative Objectives</b>				
Reduction of False Alarms	Number of false alarms eliminated at demonstrator operating point.	<ul style="list-style-type: none"> <li>• Prioritized dig list</li> <li>• Scoring report from APG</li> </ul>	Reduction of false alarms by > 50% with 95% correct identification of munitions	Yes
Location Accuracy	Average error and standard deviation in both axes for interrogated items	<ul style="list-style-type: none"> <li>• Estimated location from analysis</li> <li>• Scoring report from APG</li> </ul>	$\Delta N$ and $\Delta E < 10$ cm $\sigma N$ and $\sigma E < 15$ cm	Yes
Production Rate	Number of targets interrogated each day	<ul style="list-style-type: none"> <li>• Log of field work</li> </ul>	75 targets per day	Yes
Analysis Time	Average time required for inversion and classification	<ul style="list-style-type: none"> <li>• Log of analysis work</li> </ul>	15 min per target	Yes
<b>Qualitative Objectives</b>				
Ease of Use		<ul style="list-style-type: none"> <li>• Feedback from operator on ease of use</li> </ul>	Operator comes to work smiling	Yes

### 7.1.1 OBJECTIVE: REDUCTION OF FALSE ALARMS

This is the primary measure of the effectiveness of this technology. By collecting high-quality, precisely-located data, we expect to be able to discriminate munitions from scrap and frag with high efficiency.

#### 7.1.1.1.Metric

At a seeded test site such as the APG standardized test site, the metric for false alarm elimination is straightforward. We prepared a ranked dig list for the targets we interrogated with a dig/no-dig threshold indicated and ATC personnel use their automated scoring algorithms to assess our results.

### 7.1.1.2.Data Requirements

The identification of most of the items in the test field is known to the test site operators. Our ranked dig list is the input for this standard and ATC's standard scoring is the output.

### 7.1.1.3.Success Criteria

The objective will be considered to be met if more than 50% of the non-munitions items can be labeled as no-dig while retaining 95% of the munitions items on the dig list.

### 7.1.1.4.Results

This Objective was successfully met. The TEMTADS surveyed anomalies detected by the MTADS magnetometer system in the Blind Grid and Indirect Fire Areas. For the Blind Grid Test Area, the discrimination stage results are summarized in Table 7-2 and Table 7-3 (subsets of Table 6a of Reference 15), broken out by munitions type and emplacement depth. For the Indirect Fire Test Area, the discrimination stage results are summarized in Table 7-4 and Table 7-5 (subsets of Table 6c of Reference 15), broken out by munitions type and emplacement depth. The Discrimination Stage Probability of Detection  $P_d^{disc}$  is defined as the number of correctly identified munitions divided by the number of emplaced munitions, and the corresponding Probability of False Positive  $P_{fp}^{disc}$  is the number of clutter items incorrectly identified as munitions divided by the number of emplaced clutter items.

Table 7-2 – TEMTADS Blind Grid Test Area  $P_d^{disc}$  Results

$P_d^{disc}$	All Types	105-mm	81/60mm	37/25-mm
Munitions Scores	0.97	0.93	0.97	1.00
0 to 4D	1.00	1.00	1.00	1.00
4D to 8D	1.00	1.00	1.00	1.00
8D to 12D	0.67	0.67	0.00	1.00

Table 7-3 – TEMTADS Blind Grid Test Area  $P_{fp}^{disc}$  Results

$P_{fp}^{disc}$	All Masses	0 to 0.25 kg	>0.25 to 1 kg	>1 to 10 kg
All Depths	0.01	0.02	0.00	0.00
0 to 0.15m	0.01	0.02	0.00	0.00
0.15 to 0.3m	0.00	0.00	0.00	0.00
0.3 to 0.6m	N/A	N/A	N/A	N/A

Table 7-4 – TEMTADS Indirect Fire Test Area  $P_d^{disc}$  Results

$P_d^{disc}$	All Types	105-mm	81/60mm	37/25-mm
Munitions Scores	0.92	0.93	0.93	0.91
By Density				
High	0.88	0.92	0.91	0.80
Medium	0.94	0.97	0.89	0.97
Low	0.94	0.90	0.97	0.94
By Depth				
0 to 4D	0.96	0.94	0.97	0.97
4D to 8D	0.92	0.94	0.92	0.86
8D to 12D	0.72	0.75	0.78	0.67

Table 7-5 – TEMTADS Indirect Fire Test Area  $P_{fp}^{disc}$  Results

$P_{fp}^{disc}$	All Masses	0 to 0.25 kg	>0.25 to 1 kg	>1 to 10 kg
All Depths	0.04	0.03	0.02	0.11
0 to 0.15m	0.04	0.04	0.02	0.13
0.15 to 0.3m	0.04	0.00	0.06	0.06
0.3 to 0.6m	0.08	0.00	0.00	0.20

Discrimination Efficiency (E) and False Positive Rejection Rate ( $R_{fp}$ ) measure the effectiveness of the discrimination stage processing. The goal of discrimination is to retain the greatest number of munitions detections from the anomaly list, while rejecting the maximum number of anomalies arising from non-munitions items. Efficiency measures the fraction of detected munitions retained after discrimination, while the rejection rate measures the fraction of false alarms rejected. The measures are defined relative to the number of munitions items or the number of clutter items that were actually detected by the sensor. The results for the Blind Grid and Indirect Fire Test Areas are summarized in Table 7-6 and Table 7-7, from Tables 7a and 7c of Reference 15. Performance levels are shown at two specific operating points on the ROC curve: one at the point where no decrease in  $P_d$  is incurred and the other at the operator-selected operating point or threshold. In the Blind Grid, 98% of the emplaced munitions items were detected. Of these, 99% (97% of the emplaced munitions) were correctly classified at our selected operating point, with a corresponding false positive rejection rate of 99%. Moving out the ROC to the point where 100% of the detected munitions items are correctly classified reduces the false positive rejection rate to 95%. In the Indirect Fire Area, 94% of the emplaced munitions were detected, and 92% of the emplaced munitions were correctly classified, resulting in a discrimination efficiency of 98%. The corresponding false positive rejection rate was 92%.

Table 7-6 – TEMTADS Blind Grid Test Area Efficiency and Rejection Rates

	<b>Efficiency (E)</b>	<b>False Positive Rejection Rate</b>
At Operating Point	0.99	0.99
With No Loss of $P_d$	1.00	0.95

Table 7-7 – TEMTADS Indirect Fire Test Area Efficiency and Rejection Rates

	<b>Efficiency (E)</b>	<b>False Positive Rejection Rate</b>
At Operating Point	0.98	0.92
With No Loss of $P_d$	1.00	0.58

## 7.1.2 OBJECTIVE: LOCATION ACCURACY

An important measure of how efficiently any required remediation will proceed is the accuracy of predicted location of the targets marked to be dug. Large location errors lead to confusion among the UXO techs assigned to the remediation costing time and often leading to removal of a small, shallow object when a larger, deeper object was the intended target.

### 7.1.2.1.Metric

As above, the metric for location accuracy is straightforward at a seeded test site such as the APG standardized test site. We provided an estimated position for all targets we interrogated and ATC personnel used their automated scoring algorithms to assess our results.

### 7.1.2.2.Data Requirements

The location of most of the items in the test field is known to the test site operators. Our dig list is the input for this standard and ATC's standard scoring is the output.

### 7.1.2.3.Success Criteria

The objective will be considered to be met if the average position error was less than 10 cm in both dimensions (low bias) and the standard deviation of each dimension was less than 15 cm (accurate location).

#### 7.1.2.4.Results

This Objective was successfully met. The location accuracy of fit parameters generated from the TEMTADS array data are given in Table 7-8 and Table 7-9, taken from Tables 9a and 9c of Reference 15. Horizontal errors are not calculated for the Blind Grid.

Table 7-8 – TEMTADS Blind Grid Test Area Location Error and Standard Deviation

	<b>Mean (m)</b>	<b>Standard Deviation (m)</b>
Northing	N/A	N/A
Easting	N/A	N/A
Depth	0.02	0.04

Table 7-9 – TEMTADS Indirect Fire Test Area Location Error and Standard Deviation

	<b>Mean (m)</b>	<b>Standard Deviation (m)</b>
Northing	0.01	0.05
Easting	0.01	0.05
Depth	0.00	0.06

### 7.1.3 OBJECTIVE: PRODUCTION RATE

Even if the performance of the technology on the two metrics above is satisfactory, there is an economic metric to consider. There is a known cost of remediating a suspected munitions item. If the cost to interrogate a target is greater than this cost, the technology will be useful only at sites with special conditions or target values. Note, however, that in its ultimate implementation this technology will result in reacquisition, cued interrogation, and target flagging in one visit to the site.

#### 7.1.3.1.Metric

The number of targets interrogated per day is the metric for this objective. Combined with the daily operating cost of the technology this gives the per-item cost.

#### 7.1.3.2.Data Requirements

Survey productivity was determined from a review of the ATC demonstration field logs.

### **7.1.3.3.Success Criteria**

For this first demonstration, the objective will be considered to be met if at least 75 targets were interrogated each survey day.

### **7.1.3.4.Results**

This Objective was successfully met. Data collection times are taken from Table 5 of Reference 15. For the purposes of this discussion, a typical work day is assumed to be 7 hours of active data collection and 1 hour of daily setup and tear down. 214 anomalies were investigated on the Blind Grid over the course of 10 hours and 3 minutes, or 1.43 work days, or on average 149 anomalies / work day. 694 anomalies were investigated in the Indirect Fire Area over the course of 32 hours and 30 minutes, or on average 150 anomalies / work day. In fact, through the generosity of the ATC staff, we were able to work for ten or more hours on several days and achieved production rates of > 220 anomalies / day for three days at the end of the first week of the demonstration.

## **7.1.4 OBJECTIVE: ANALYSIS TIME**

The ultimate implementation of this technology will involve on-the-fly analysis and classification. The time for this will be limited to the driving time to the next anomaly on the list. We tracked the near-real-time analysis time in this demonstration.

### **7.1.4.1.Metric**

The time required for inversion and classification per anomaly is the metric for this objective

### **7.1.4.2.Data Requirements**

Analysis time will be determined from a review of the data analysis logs.

### **7.1.4.3.Success Criteria**

For this first demonstration, the objective will be considered to be met if the average inversion and classification time was less than 15 min.

### **7.1.4.4.Results**

This Objective was successfully met. The average inversion time per target was approximately 2.5 minutes on our field laptop computer. Including this, the average analysis time amounted to 12.5 minutes per anomaly. Since this was the first extensive test of the system in field mode, we took the opportunity to consider various discrimination and classification methods, some of which proved unfruitful. As a result of lessons learned from this undertaking, we expect the average analysis time for future field runs to be less than that obtained here.

### **7.1.5 OBJECTIVE: EASE OF USE**

This qualitative objective is intended as a measure of the long-term usability of the technology. If the operator does not report that the technology is easy to use, shortcuts that can compromise the efficiency of the technology will begin to creep into daily operations.

#### **7.1.5.1.Data Requirements**

This objective was evaluated based on operator feedback.

#### **7.1.5.2.Results**

This Objective was successfully met. Based on vehicle operator feedback, there were no significant limitations to the efficient use of the system in the field. Several suggestions were made for additional improvements to the navigation and data collection software. They have been subsequently incorporated. Anomalies for future demonstrations will be ordered along 1m swaths for maximum data collection efficiency.

## **7.2 FORMER CAMP SAN LUIS OBISPO**

The performance objectives for the demonstration were presented in Table 3-2, and are repeated here as Table 7-10.

Prior to our demonstration run at the former Camp SLO, we obtained measurements of each of the four munitions types. Using the derived polarizabilities from these measurements and the forward model of our TEMTADS code, response curves were generated for each munition. These curves plot the minimum expected peak signal (the peak signal when the target is oriented horizontally) and the maximum expected peak (the peak signal when the target is oriented horizontally) from each target as a function of distance below sensor or depth below ground. The peak signal is that obtained from the monostatic term of the center element of the array at the first time gate.

A calibration strip, comprised of two samples of each of the four targets of interest plus two shotputs (Table 7-11), was emplaced on site as a means of verifying proper system operation on a daily basis. The strip was surveyed twice daily, once at the beginning of the day, and once at the end. The sole exception to this procedure occurred on our third day, when brake problems with the vehicle forced an early cessation of activities.

Table 7-10 – Performance Objectives for the former Camp SLO Demonstration

Performance Objective	Metric	Data Required	Success Criteria	Success?
Site Coverage	Fraction of assigned anomalies interrogated	Survey results	100% as allowed for by topography / vegetation	Yes
Calibration Strip Results	System response consistently matches physics-based model	<ul style="list-style-type: none"> <li>• System response curves</li> <li>• Daily calibration strip data</li> </ul>	<ul style="list-style-type: none"> <li>• <math>\leq 15\%</math> rms variation in amplitude</li> <li>• Down-track location <math>\pm 25\text{cm}</math></li> <li>• All response values fall within bounding curves</li> </ul>	No
Location Accuracy	Average error and standard deviation in both axes for interrogated items	<ul style="list-style-type: none"> <li>• Estimated location from analyses</li> <li>• Ground truth from validation effort</li> </ul>	$\Delta N$ and $\Delta E < 5\text{ cm}$ $\sigma N$ and $\sigma E < 10\text{ cm}$	No
Depth Accuracy	Standard deviation in depth for interrogated items	<ul style="list-style-type: none"> <li>• Estimated location from analyses</li> <li>• Ground truth from validation effort</li> </ul>	$\Delta \text{Depth} < 5\text{ cm}$ $\sigma \text{Depth} < 10\text{ cm}$	No
Production Rate	Number of anomalies investigated each day	<ul style="list-style-type: none"> <li>• Survey results</li> <li>• Log of field work</li> </ul>	125 anomalies/day	Yes
Data Throughput	Throughput of data QC process	Log of analysis work	All data QC'ed on site and at pace with survey	Yes
Reliability and Robustness	General Observations	Team feedback	Field team comes to work smiling	Yes

Table 7-11 – Details of former Camp SLO Calibration Strip

Item ID	Description	Easting (m)	Northing (m)	Depth (m)	Inclination	Azimuth (°cw from N)
T-001	shotput	705,417.00	3,913,682.00	0.25	N/A	N/A
T-002	81mm	705,420.92	3,913,687.63	0.30	Vertical Down	0
T-003	81mm	705,424.10	3,913,692.95	0.30	Horizontal	120
T-004	60mm	705,427.53	3,913,698.54	0.30	Vertical Down	0
T-005	60mm	705,430.85	3,913,704.10	0.30	Horizontal	120
T-006	4.2” mortar	705,434.54	3,913,709.44	0.30	Vertical Down	0
T-007	4.2” mortar	705,437.99	3,913,715.04	0.30	Horizontal	120
T-008	2.36” rocket	705,441.46	3,913,720.24	0.30	Vertical Down	0
T-009	2.36” rocket	705,445.00	3,913,725.91	0.30	Horizontal	120
T-010	shotput	705,448.50	3,913,731.50	0.35	N/A	N/A

## 7.2.1 OBJECTIVE: SITE COVERAGE

A list of previously identified anomalies was provided by the Program Office.

### 7.2.1.1.Metric

Site coverage is defined as the fraction of the assigned anomalies surveyed by the TEMTADS.

### 7.2.1.2.Data Requirements

The collected data were compared to the original anomaly list. All interferences were noted in the field log book.

### 7.2.1.3.Success Criteria

The objective was considered met if 100% of the assigned anomalies are surveyed with the exception of areas that can not be surveyed due to topology / vegetation interferences.

### 7.2.1.4.Results

This objective was successfully met. Of the list provided by the Program Office, all but 5 were measured. Failure to measure these 5 anomalies was due to the presence of rocks which prevented the operator from positioning the TEMTADS over the target.

## 7.2.2 OBJECTIVE: CALIBRATION STRIP RESULTS

This objective supports that each sensor system is in good working order and collecting physically valid data each day. The calibration strip was surveyed twice daily. The peak

positive response of each emplaced item from each run was compared to the physics-based response curves generated prior to data collection on site using each item of interest.

#### **7.2.2.1.Metric**

The reproducibility of the measured response of each sensor system to the items of interest and the comparison of the response to the response predicted by the physics-based model defines this metric.

#### **7.2.2.2.Data Requirements**

Response curves for each sensor / item of interest pair are used to document what the physics-based response of the system to the item should be. The tabulated peak response values from each survey of the Calibration Strip demonstrates the reproducibility and validity of the sensor readings.

#### **7.2.2.3.Success Criteria**

The objective is considered met if all measured responses fall within the range of physically possible values based on the appropriate response curve. Additionally, the RMS variation in responses should be less than 15% of the measured response and the down-track location of the anomaly should be within 25 cm of the corresponding seeded item's true location.

#### **7.2.2.4.Results**

This objective was not successfully met in full. The measured peak signals for all of the emplaced items are shown in Figure 7-1 through Figure 7-5. The maximum (red) and minimum (blue) response curves are plotted for all objects except the shotput, which has only one curve due to symmetry. The two curves for the 81-mm and 4.2-in mortar are nearly equal. For self-consistency, we have plotted the measurements at the mean inverted depth, rather than the reported depths. The measured values generally fit well within the bounding curves, with the 4.2-in mortar and shotput results the poorest, with a tendency to underestimate the peak value.

Careful examination of the data shows that this variation is the result of the shot-to-shot precision with which the array can be positioned in exactly the same spot each time. Because the response curves are generated assuming the target is directly below the sensor, any offset in the sensor position will result in the derived peak signal being smaller than that predicted by the curve, as is observed. For future demonstrations, the metric of polarizability amplitude is recommended as these values are invariant to array position.

Table 7-12 shows the mean and standard deviation in the peak measured signal for all of the emplaced Calibration Strip items. Of the 10 items, three give RMS variations above our stated goal of 15%, with only T-008 being significantly above. This target consistently inverted to a depth of 18.5 cm, and thus showed the largest spatial variation in signal. This, coupled with the

array not always being properly centered on the target, explains the larger variation for this object.

Table 7-12 – Peak Signals for former Camp SLO Calibration Strip Emplaced Items

Item ID	Description	Depth (m)	Mean Signal (mV/Amp)	Std Dev. (mV/Amp,1 $\sigma$ )	Variation (%)
T-001	shotput	0.25	27.44	4.18	15.23
T-002	81mm	0.30	15.46	1.39	8.99
T-003	81mm	0.30	10.96	0.91	8.30
T-004	60mm	0.30	8.74	0.89	10.18
T-005	60mm	0.30	6.73	1.13	16.79
T-006	4.2" mortar	0.30	52.38	5.82	11.11
T-007	4.2" mortar	0.30	41.75	5.25	12.57
T-008	2.36" rocket	0.30	32.70	7.91	24.19
T-009	2.36" rocket	0.30	4.04	0.32	7.92
T-010	shotput	0.35	11.82	1.52	12.86

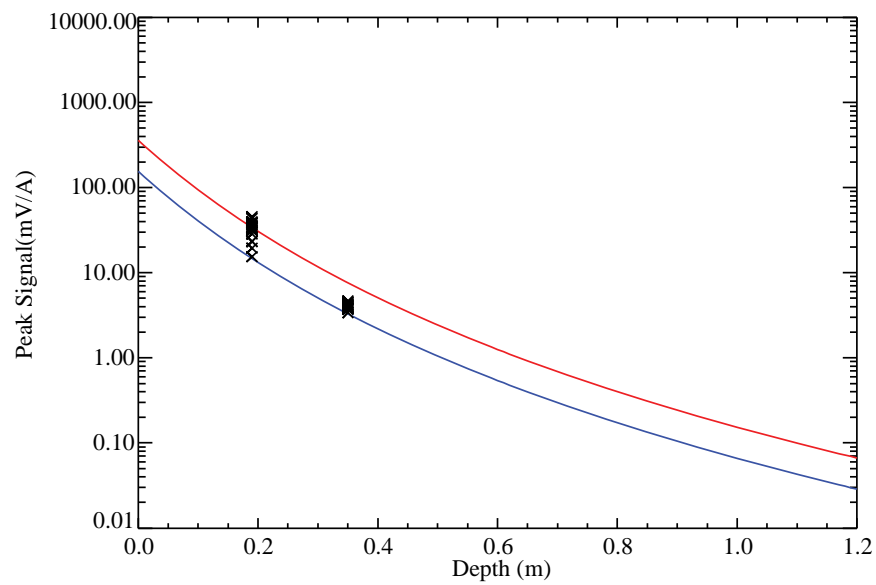


Figure 7-1 – Peak signals compared with response curve for a 2.36-in rocket.

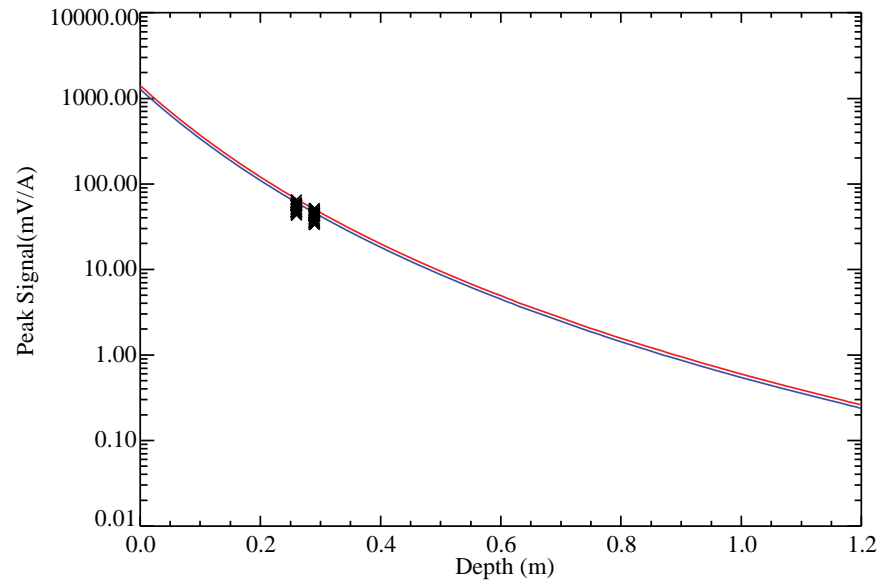


Figure 7-2 – Peak signals compared with response curve for a 4.2-in mortar.

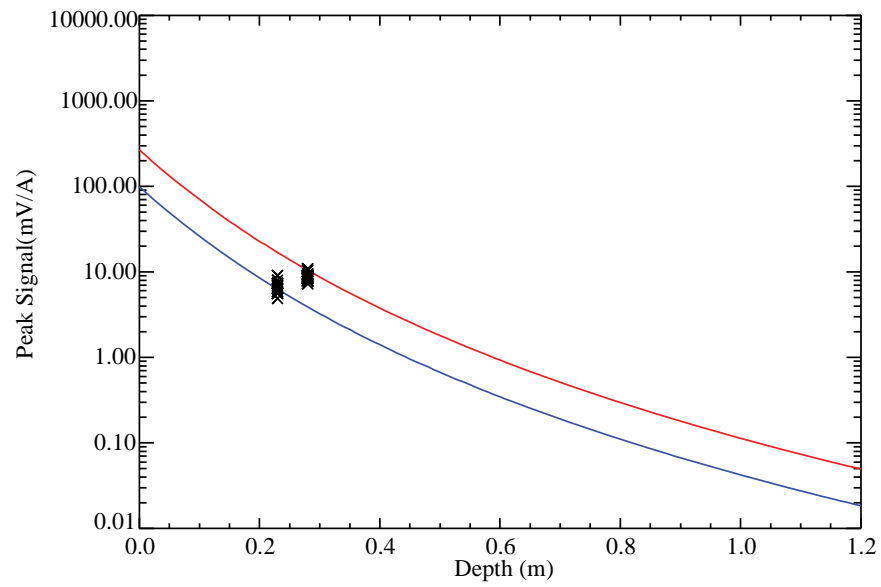


Figure 7-3 – Peak signals compared with response curve for a 60-mm mortar.

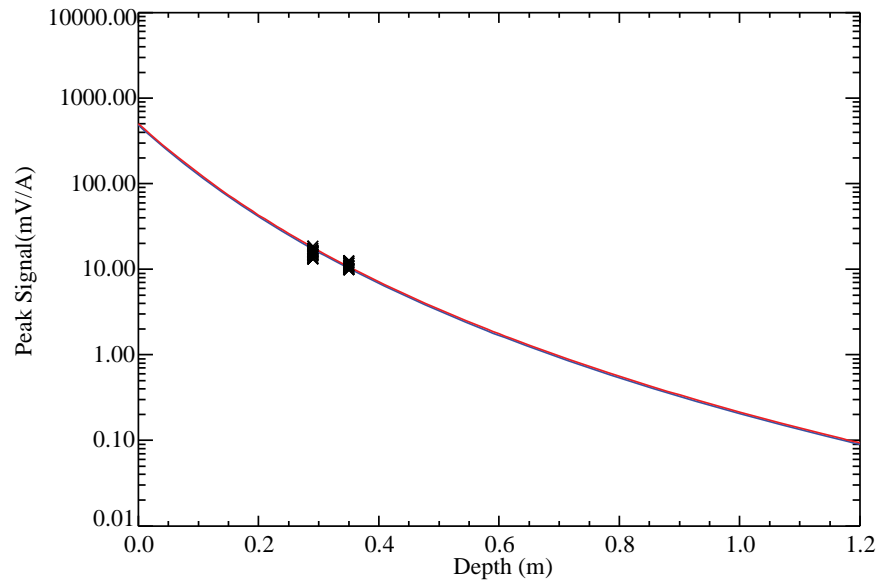


Figure 7-4 – Peak signals compared with response curve for an 81-mm mortar.

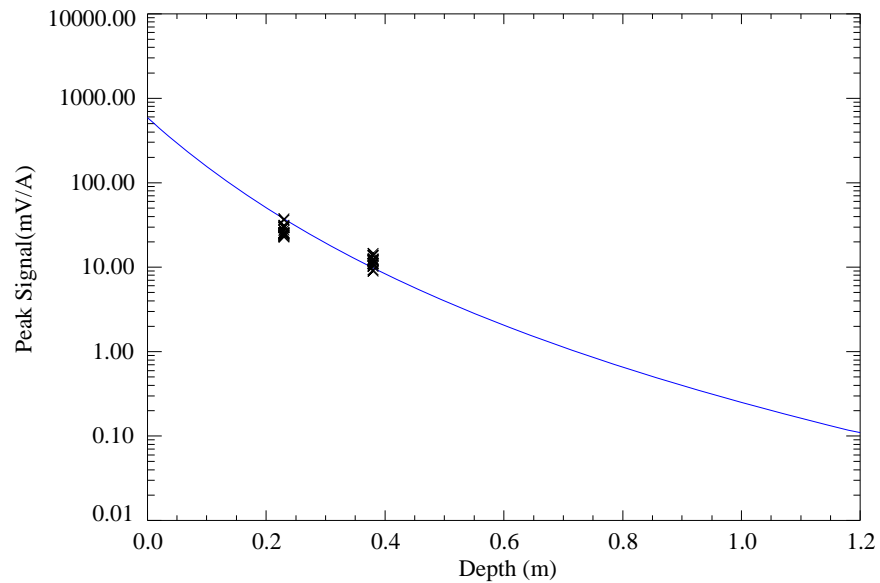


Figure 7-5 – Peak signals compared with response curve for a 4-in diameter shotput.

The variability and accuracy of the positional fit parameters for the Calibration Strip emplaced items were determined by comparing the inverted Northing and Easting values with reported values. These numbers are shown in Table 7-13. We give the mean vector offset  $dR$  between the inverted and reported position as well as the Easting ( $dx$ ) and Northing ( $dy$ ) components. The  $dx$  and  $dy$  values are computed using the inverted positions minus the reported ones.

Two points are clear from the values in Table 7-13. First, the inversion process is very robust, with no standard deviations larger than 2cm. Second, there are a few large discrepancies between our inverted positions and the reported ones. All offsets are below our target value of 25cm, with the exception of T-002. It is possible that some items have drifted or settled since their original emplacement.

Table 7-13 – Position Accuracy and Variability for former Camp SLO Calibration Strip Emplaced Items

Item ID	Description	Depth (m)	Mean dR (m)	Std Dev dR (m, 1 $\sigma$ )	Mean dx (m)	Std Dev dx (m)	Mean dy (m)	Std Dev dy (m)
T-001	shotput	0.25	0.209	0.007	0.167	0.013	0.124	0.011
T-002	81mm	0.30	0.413	0.008	-0.372	0.008	-0.178	0.010
T-003	81mm	0.30	0.058	0.014	0.028	0.010	-0.049	0.020
T-004	60mm	0.30	0.026	0.013	0.013	0.010	0.015	0.019
T-005	60mm	0.30	0.038	0.012	-0.003	0.011	0.035	0.017
T-006	4.2" mortar	0.30	0.098	0.008	0.082	0.009	0.054	0.009
T-007	4.2" mortar	0.30	0.063	0.008	0.061	0.009	0.013	0.010
T-008	2.36" rocket	0.30	0.035	0.010	-0.027	0.011	0.018	0.011
T-009	2.36" rocket	0.30	0.112	0.016	0.051	0.010	-0.099	0.018
T-010	shotput	0.35	0.166	0.006	0.133	0.008	-0.098	0.014

### 7.2.3 OBJECTIVE: LOCATION ACCURACY

An important measure of how efficiently any required remediation will proceed is the accuracy of the predicted location of the targets marked to be dug. Large location errors lead to confusion among the UXO technicians assigned to the remediation, costing time and often leading to removal of a small, shallow object when a larger, deeper object was the intended target.

#### 7.2.3.1.Metric

The average error and standard deviation in both horizontal axes will be computed for the items selected for excavation during the validation phase of the study.

#### 7.2.3.2.Data Requirements

The anomaly fit parameters and the ground truth for the excavated items are required to determine the performance of the fitting routines in terms of the location accuracy.

#### 7.2.3.3.Success Criteria

This objective is considered as met if the average error in position for both Easting and Northing quantities is less than 5 cm and the standard deviation for both is less than 10 cm.

#### **7.2.3.4.Results**

This objective was not successfully met in full. The average Northing position error for all measured data was 1.5cm, while the average Easting position error was 3cm. The standard deviations, however, were larger than desired, with both values about 25cm. Excluding those anomalies for which multiple targets were found produces negligible improvement. We suspect the higher values are due to the large number of small, low SNR clutter items, which result in greater uncertainty in both the measured and fitted values. Indeed, if we restrict ourselves to those anomalies which we classified as ‘likely UXO,’ the Northing and Easting standard deviations drop to 7cm and 5cm, respectively.

#### **7.2.4 OBJECTIVE: DEPTH ACCURACY**

An important measure of how efficiently any required remediation will proceed is the accuracy of the predicted depth of the targets marked to be dug. Large depth errors lead to confusion among the UXO technicians assigned to the remediation, costing time and often leading to removal of a small, shallow object when a larger, deeper object was the intended target.

##### **7.2.4.1.Metric**

The standard deviation of the predicted depths with respect to the ground truth will be computed for the items which are selected for excavation during the validation phase of the study.

##### **7.2.4.2.Data Requirements**

The anomaly fit parameters and the ground truth for the excavated items are required to determine the performance of the fitting routines in terms of the predicted depth accuracy.

##### **7.2.4.3.Success Criteria**

This objective is considered as met if the average error in depth is less than 5 cm and the standard deviation is less than 10 cm.

##### **7.2.4.4.Results**

This objective was not successfully met in full. The average depth error for all measured data was 2.5cm. The standard deviation was a bit larger than desired, with a value of 14cm. As we did for the Northing and Easting, we tried excluding those anomalies for which multiple targets were found. This lowered the value to 11cm. Restricting ourselves to those anomalies that we classified as ‘likely UXO,’ the standard deviation is lowered to a value of 7cm. This approach attempts to exclude the numerous, small, low SNR clutter items from the analysis.

## **7.2.5 OBJECTIVE: PRODUCTION RATE**

This objective considers a major cost driver for the collection of high-density, high-quality geophysical data, the production rate. The faster high quality data can be collected, the higher the financial return on the data collection effort.

### **7.2.5.1.Metric**

The number of anomalies investigated per day determines the production rate for a cued survey system.

### **7.2.5.2.Data Requirements**

The metric can be determined from the combination of the field logs and the survey results. The field logs record the amount of time per day spent acquiring the data and the survey results determine the number of anomalies investigated in that time period.

### **7.2.5.3.Success Criteria**

This objective is considered met if average production rate is at least 125 anomalies / day.

### **7.2.5.4.Results**

This objective was successfully met. A total of 1547 anomalies (including redo's) were measured over a 10-day run for an average of 155 anomalies/day. The only days for which our average fell below our goal of 125 anomalies/day were the final day, due to finishing up all targets, and 2 days in which necessary vehicle repairs shortened our workday.

## **7.2.6 OBJECTIVE: DATA THROUGHPUT**

The collection of a complete, high-quality data set with the sensor platform is critical to the downstream success of the UXO Classification Study. This objective considers one of the key data quality issues, the ability of the data analysis workflow to support the data collection effort in a timely fashion. To maximize the efficient collection of high quality data, a series of MTADS standard data quality check are conducted during and immediately after data collection on site. Data which pass the QC screen are then processed into archival data stores. Individual anomaly analyses were then conducted on those archival data stores. The data QC / preprocessing portion of the workflow needs to keep pace with the data collection effort for best performance.

### **7.2.6.1.Metric**

The throughput of the data quality control workflow is at least as fast the data collection process, providing real time feedback to the data collection team of any issues.

#### **7.2.6.2.Data Requirements**

The data analyst's log books will provide the necessary data for determining the success of this metric.

#### **7.2.6.3.Success Criteria**

This objective is considered met if all collected data can be processed through the data quality control portion of the workflow in a timely fashion.

#### **7.2.6.4.Results**

This objective was successfully met. Data were normally downloaded several times during each workday, and quality control on these datasets was usually completed on the same day. Quality control checks successfully caught missed anomalies, a small number of corrupt data files, and targets which needed re-measuring.

### **7.2.7 OBJECTIVE: RELIABILITY AND ROBUSTNESS**

This objective represents an opportunity for all parties involved in the data collection process, especially the vehicle operator, to provide feedback on areas where the process could be improved.

#### **7.2.7.1.Data Requirements**

This decision was based on verbal discussions, communications, and opinions of the entire field team.

#### **7.2.7.2.Results**

This objective was successfully met. Based on vehicle operator feedback, there were no significant limitations to the efficient use of the system in the field.

## **8.0 COST ASSESSMENT**

The costs for a 3,000 anomaly cued survey using the TEMTADS are detailed in Table 8-1. The costs associated with the former Camp SLO demonstration were used as the basis for this assessment. The costs reported here do not include any costs associated with the reconnaissance data that were used to identify and create the cued list of anomalies. Implicit in our assessment is that the 3,000 anomalies are bounded within an area of roughly 25 acres, or 120 anomalies/acre. Survey time would increase incrementally as the anomaly density decreased as transit time between anomalies increased. All costs are estimated in FY 2009 dollars.

## **8.1 COST MODEL**

A cost model was constructed from the costs associated with the TEMTADS survey of the former Camp SLO demonstration site. Cost categories were mobilization, logistics (if required), field work, demobilization, data analysis, and reporting. Based on the demonstrated production rate for the former Camp SLO demonstration, four weeks of field work would be required. Based on the production rate for the APG demonstration, the SLO production rate is a conservative lower bound. This model does not include the cost of anomaly classification and producing a prioritized dig list.

Table 8-1 – Summary of Costs for a 25-acre, 3000 anomaly TEMTADS survey.

Cost Category	Sub-Category	Cost	Sub-Total
Mobilization Costs			\$44,550
	Preliminary Site Visit	\$6,500	
	Test Plan Preparation	\$10,250	
	Equipment Prep and Packing	\$9,750	
	53' Trailer Transportation	\$5,800	
	Analysts Set-up	\$10,000	
	Outbound Travel for 3 Personnel	\$2,250	
Logistics (if required)			\$16,500
	Establish GPS Control Points	\$2,000	
	Delivery/Removal of Logistics Items	\$2,000	
	Rental of Logistics Items / Fuel	\$6,000	
	Materials	\$6,500	
Operating Costs (4-week Survey)			\$139,050
	Supervisor	\$19,000	
	On-site Analyst	\$31,800	
	Vehicle Operator	\$12,750	
	Field Technician (2 each)	\$17,250	
	Per Diem (3 Personnel x 4 weeks x \$1250)	\$15,000	
	Rental Vehicles	\$8,650	
	System Maintenance	\$13,000	
	Sensor Repair	\$21,600	
Analysis & Reporting			\$44,750
	Data Reduction to Anomaly List	\$28,000	
	Demonstration Data Report	\$16,750	
Demobilization Costs			\$11,550
	Equipment Unpacking	\$3,500	
	53' Trailer Transportation	\$5,800	
	Inbound Travel for 3 Personnel	\$2,250	
Total Cost			\$256,400

## **8.2 COST DRIVERS**

Two factors were expected to be strong drivers of cost for this technology as demonstrated. The first is the number of anomalies which can be surveyed per day. Higher productivity in data collection equates to more anomalies investigated for a given period of time in the field. The time required for analyzing individual anomalies can be significantly higher than for other, more traditional methods and could become a cost driver due to the time involvement. The thoughtful use of available automation techniques for individual anomaly analysis with operator QC support can moderate this effect.

## **8.3 COST BENEFIT**

The main benefit to using a UXO classification process is cost-related. The ability to reduce the number of non-hazardous items that have to be dug or dug as hazardous directly reduces the cost of a remediation effort. The additional information for anomaly classification provided by the TEMTADS array provides additional information for the purposes of anomaly classification. If there is buy-in from the stakeholders to use these techniques, this information can be used to reduce costs.

## **9.0 IMPLEMENTATION ISSUES**

Implementation issues for this system / technology fall into two categories: operational concerns and data quality / analysis issues. In terms of operational concerns, the TEMTADS as implemented is a large, vehicle-towed system that operates best in large, open areas. As seen at the former Camp SLO demonstration, it is possible to operate the system in rocky terrain with grades approaching 20%, but at reduced operating capacity and increased system wear. Smaller versions of the system are currently under development under several ESTCP and SERDP projects to address these concerns. The goal is to design and field units more amenable to operation in more confined terrain and topology and smaller tow vehicles / man-portable and handheld operation. In terms of data quality, one pays a small penalty in signal amplitude to use the smaller TEMTADS sensor coil as compared to other systems such as a high-power EM61 MkII. The dramatically improved electrical performance of these new sensors helps counterbalance this issue, particularly in the ability to perform better averaging (or stacking). However, one needs in place robust data QC techniques to know when to employ these capabilities in an efficient manner.

## 10.0 REFERENCES

1. "Report of the Defense Science Board Task Force on Unexploded Ordnance," December 2003, Office of the Under Secretary of Defense for Acquisition, Technology, and Logistics, Washington, D.C. 20301-3140, <http://www.acq.osd.mil/dsb/uxo.pdf>.
2. <http://aec.army.mil/usaec/technology/jpgphaseiv.pdf>.
3. "Standardized UXO Technology Demonstration Site Blind Grid Scoring Record No. 39," <http://aec.army.mil/usaec/technology/uxo-record39.pdf>.
4. Foley, J. E., M. Miele, R. Mehl, J. Dolynchuk, J. Hodgson and J. Swanson, "Procedures for Applying UXO Discrimination Technology at the Former Lowry Bombing and Gunnery Range," UXO/Countermine Forum, Saint Louis, March 9-12, 2004.
5. Aberdeen Proving Ground Soil Survey Report, October 1998.
6. Nelson, H. H. and Steinhurst, D. A., "MTADS Geophysical Survey of the ATC Standardized UXO Technology Demonstration Site Proposed Active Response Area," Naval Research Laboratory Letter Report Number 6110-089, August 6, 2003.
7. "Final Site Inspection Report, Former Camp San Luis Obispo, San Luis Obispo, CA," Parsons, Inc., September 2007.
8. "Survey Control, Former Camp San Luis, Obispo," August 18, 2008.
9. Harbaugh, G.R., Kingdon, J.B., Furuya, T., Bell, T.H., and Steinhurst, D.A., "EMI Array for Cued UXO Discrimination, ESTCP MM-0601, Demonstration Data Report, APG Standardized UXO Test Site," Naval Research Laboratory Memorandum Report NRL/MR/6110--10-9234, January 14, 2010.
10. Harbaugh, G.R., Steinhurst, D.A., and Khadr, N., "ESTCP MM-0744, Demonstration Data Report, Former Camp San Luis Obispo, Magnetometer and EM61 MkII Surveys," May 7, 2010.
11. Steinhurst, D., Khadr, N., Barrow, B., and Nelson, H. "Moving Platform Orientation for an Unexploded Ordnance Discrimination System," GPS World, 2005, 16/5, 28 – 34.
12. Nelson, H. H., "Array Specification Report," ESTCP MM-0601, June, 2007.
13. Nelson, H. H., ESTCP In-Progress Review, Project MM-0601, March 1, 2007.

14. Nelson, H. H. and Robertson, R., "Design and Construction of the NRL Baseline Ordnance Classification Test Site at Blossom Point," Naval Research Laboratory Memorandum Report NRL/MR/6110—00-8437, March 20, 2000.
15. "STANDARDIZED UXO TECHNOLOGY DEMONSTRATION SITE SCORING RECORD NO. 920 (NRL)," J.S. McClung, ATC-9843, Aberdeen Test Center, MD, November, 2008.
16. Bell, T., Barrow, B., Miller, J., and Keiswetter, D., "Time and Frequency Domain Electromagnetic Induction Signatures of Unexploded Ordnance," Subsurface Sensing Technologies and Applications Vol. 2, No. 3, July 2001.
17. Bell, T. H., Barrow, B. J., and Miller, J. T., "Subsurface Discrimination Using Electromagnetic Induction Sensors," IEEE Transactions on Geoscience and Remote Sensing, Vol. 39, No. 6, June 2001.
18. SAIC Analysis of Survey Data Acquired At Camp Sibert, ESTCP MM-0210 Interim Report, July 14, 2008.
19. Kingdon, J.B., Harbaugh, G.R., Steinhurst, D.A., Bell, T.H., and Keiswetter, D.A, "ESTCP MM-0744, Data Collection Report, Former Camp San Luis Obispo, EMI Array for Cued UXO Discrimination," May 7, 2010.

## Appendix A: Points of Contact

<b>POINT OF CONTACT</b>	<b>ORGANIZATION</b>	<b>Phone Fax e-mail</b>	<b>Role in Project</b>
Dr. Jeff Marqusee	ESTCP Program Office 901 North Stuart Street, Suite 303 Arlington, VA 22203	703-696-2120 (V) 703-696-2114 (F) jeffrey.marqusee@osd.mil	Director, ESTCP
Dr. Anne Andrews	ESTCP Program Office 901 North Stuart Street, Suite 303 Arlington, VA 22203	703-696-3826 (V) 703-696-2114 (F) anne.andrews@osd.mil	Deputy Director, ESTCP
Dr. Herb Nelson	ESTCP Program Office 901 North Stuart Street, Suite 303 Arlington, VA 22203	703-696-3726 (V) 703-696-2114 (F) 202-215-4844 (C) herbert.nelson@osd.mil	Program Manager, MM
Mr. Peter Knowles	HydroGeoLogic, Inc. 11107 Sunset Hills Road, Suite 400 Reston, VA 20190	703-736-4511 (V) pknowles@hgl.com	Program Manager's Assistant, MM
Dr. Dan Steinhurst	Naval Research Lab Chemistry Division Code 6110 Washington, DC 20375	202-767-3556 (V) 202-404-8119 (F) 703-850-5217 (C) dan.steinhurst@nrl.navy.mil	Co-PI and Data Analyst
Dr. Tom Bell	SAIC 200 12th Street South Arlington, VA 22202	703-414-3904 (V) 703-413-0505 (F) 301-712-7021 (C) thomas.h.bell@saic.com	Co-PI and Quality Control Officer
Mr. Rick Fling	Aberdeen Test Center	410-278-2999 (V) 301-992-9080 (C) rick.fling@us.army.mil	Test Site Manager
Mr. David Ragsdale	California Polytechnic State University San Luis Obispo, CA 93407	805-756-6662 (V) 805-756-1602 (F) dragsdal@calpoly.edu	Environmental Health & Safety Manager / Risk Management